Mitotic phosphorylation of Exo84 disrupts exocyst assembly and arrests cell growth

Guangzuo Luo,[1] Jian Zhang,[1] Francis C. Luca,[2] and Wei Guo[1]

[1]Department of Biology, School of Arts and Sciences, and [2]Department of Animal Biology, School of Veterinary Medicine, University of Pennsylvania, Philadelphia, PA 19104

The rate of eukaryotic cell growth is tightly controlled for proper progression through each cell cycle stage and is important for cell size homeostasis. It was previously shown that cell growth is inhibited during mitosis when cells are preparing for division. However, the mechanism for growth arrest at this stage is unknown. Here we demonstrate that exocytosis of a select group of cargoes was inhibited before the metaphase–anaphase transition in the budding yeast *Saccharomyces cerevisiae*. The cyclin-dependent kinase, Cdk1, when bound to the mitotic cyclin Clb2, directly phosphorylated Exo84, a component of the exocyst complex essential for exocytosis. Mitotic phosphorylation of Exo84 disrupted the assembly of the exocyst complex, thereby affecting exocytosis and cell surface expansion. Our study demonstrates the coordination between membrane trafficking and cell cycle progression and provides a molecular mechanism by which cell growth is controlled during the cell division cycle.

Introduction

The rate of cell growth is tightly controlled at different stages of the cell cycle for accurate reproduction and cell size homeostasis (Jorgensen and Tyers, 2004). It was shown more than 50 years ago that cell growth dramatically decreases during mitosis in mammalian cells (Prescott and Bender, 1962). Cell surface expansion decreases as cells approach metaphase and recover after the metaphase–anaphase transition (Boucrot and Kirchhausen, 2007, 2008). Similarly, fission and budding yeast cell growth, as measured by cell volume and surface expansion, decreases during mitosis (Mitchison and Nurse, 1985; Goranov et al., 2009; Tzur et al., 2009). The mitotic growth arrest is thought to help cells to reorganize their structure and adapt to the increased energy demands needed for subsequent cell division or regeneration (Goranov and Amon, 2010). Despite these observations over the years, surprisingly little is known about the molecular mechanisms that arrest cell growth during mitosis.

It has been recognized since early years that membrane trafficking involving endocytosis and exocytosis controls cell surface growth during the cell cycle (Erickson and Trinkaus, 1976). Cell surface expansion is ultimately performed through exocytosis, in which post-Golgi secretory vesicles carrying proteins and lipids are docked to and fused with the plasma membrane (Boucrot and Kirchhausen, 2007). The exocyst complex, composed of Sec3, Sec5, Sec6, Sec8, Sec10, Sec15, Exo70, and Exo84, is essential for exocytosis and cell surface expansion. The dynamic assembly of the exocyst complex links the secretory vesicles and the plasma membrane in a process called "tethering," which takes place before SNARE-mediated membrane fusion (Guo et al., 2000; Whyte and Munro, 2002; Hsu et al., 2004; Munson and Novick, 2006; He and Guo, 2009). Components of the exocyst complex have been shown to be direct targets of many signaling molecules that spatially or temporally regulate exocytosis for various physiological processes such as polarized yeast cell growth, epithelia formation, neuronal branching, and cell migration (Nelson and Yeaman, 2001; Bryant and Mostov, 2008; He and Guo, 2009; Hall and Lalli, 2010; Liu and Guo, 2012).

The cyclin-dependent kinases (CDKs) are master regulators of the cell cycle and are likely to play central roles in growth control during the cell cycle (Goranov and Amon, 2010). Using the budding yeast *Saccharomyces cerevisiae*, we demonstrate that Cdk1 is a regulator of exocytosis during cell cycle progression. When bound to the mitotic cyclin Clb2, Cdk1 inhibits exocytosis before the metaphase–anaphase transition. The effect of Cdk1 is mediated by its direct phosphorylation of one of the

Correspondence to Wei Guo: guowei@sas.upenn.edu

Abbreviations used in this paper: ADH, alcohol dehydrogenase; APC, anaphase promotion complex.

The Rockefeller University Press $30.00
J. Cell Biol. Vol. 202 No. 1 97–111
www.jcb.org/cgi/doi/10.1083/jcb.201211093

exocyst components, Exo84. We further show that Exo84 phosphorylation disrupts the assembly of the exocyst complex during mitosis, thereby negatively affecting exocytosis and cell surface expansion. Our study provides a molecular mechanism by which exocytosis and cell growth is controlled during mitosis.

Results

Exocytosis is inhibited in metaphase-arrested cells

Cell growth and surface expansion are mediated by exocytosis. To examine whether exocytosis is cell cycle regulated, we monitored the secretion of endo-β-1,3-glucanase (Bgl2), a cell wall remodeling enzyme and a commonly used exocytosis marker (Harsay and Bretscher, 1995), in an array of cell cycle mutants. As shown in Fig. 1 (A and B), the intracellular Bgl2 level was elevated in the metaphase-arrested *cdc20-1* mutant, but not in the wild-type or *cdc28-4*, *cdc7-1*, and *cdc15-2* mutants, which were arrested at G1 phase, S phase, and anaphase, respectively. Cdc20 is a cofactor for the anaphase promotion complex (APC) that promotes mitotic exit by degrading mitotic cyclins and the anaphase inhibitor securin (Zachariae and Nasmyth, 1999). When transferred to the restrictive temperature (37°C), the *cdc20-1* cells arrest at metaphase with high mitotic cyclin-dependent kinase (Cdk1) activity (Lim et al., 1998). In addition to *cdc20-1*, we also tested another metaphase-arrested mutant, *cdc23-1*. Cdc23 is a subunit of APC (Zachariae and Nasmyth, 1999). The intracellular Bgl2 level was increased in the *cdc23-1* mutant at the restrictive temperature (Fig. S1 A).

In addition to the Bgl2 secretions assay, we have also examined the secretion of the *cdc* mutants using the invertase, which marks a smaller branch of the exocytic routes (Harsay and Bretscher, 1995). We found that none of the mutant strains had invertase secretion block (Fig. S1 B). The result is consistent with the previous observation (Makarow, 1988).

We have also investigated whether the secretion of glycoproteins into the media was affected in *cdc* mutants. The wild-type and *cdc* mutant cells were shifted from 25 to 37°C for 90 min. Cells were washed and resuspended in fresh medium prewarmed to 37°C. Glycoproteins secreted into the medium were precipitated by trichloroacetic acid and subjected to SDS-PAGE. The gel was then stained with Schiff's reagent, which recognizes the glycoproteins (Zhang et al., 2005). The *sec6-4* strain defective in exocytosis was used as a control. As expected, *sec6-4* displayed very weak glycoprotein staining compared with the wild-type strain (Fig. 1, C and D). The staining patterns of *cdc28-4*, *cdc7-1*, and *cdc15-2* were similar to that of the wild-type cells. The *cdc20-1* mutant, however, showed a special staining pattern, with several glycoproteins selectively missing. The secretion of a similar set of glycoproteins was affected in other experiments, as described later. This result, together with the analyses of Bgl2 secretion and invertase secretion described for *cdc* mutants, suggests that some of the exocytic pathways are specifically blocked in the *cdc20-1* mutant.

A more definitive test for a secretion block is to examine whether secretory vesicles are accumulated in the cell. We thus examined *cdc20-1* cells using thin-section EM. Secretory vesicles were barely detectable in the wild-type cells (Fig. 1, E and F). In contrast, there was a clear accumulation of vesicles (109 ± 38 vesicles per section) in the *cdc20-1* cells arrested at the metaphase at 37°C. The sizes of the accumulated vesicles ranged from 80 to 100 nm in diameter, which is characteristic of post-Golgi secretory vesicles (Novick et al., 1980). These data indicate that exocytosis is affected in metaphase-arrested *cdc20-1* cells.

In addition to the *cdc20-1* mutant, the cell cycle can also be arrested at metaphase by prolonged treatment with nocodazole, which disrupts the microtubules (Quinlan et al., 1980; Holm et al., 1985). We have examined the secretion profile of cells arrested at metaphase after 3 h of nocodazole treatment. Consistent with the previous observation by Makarow (1988), invertase secretion was not affected (Fig. S2 A). However, Bgl2 secretion was defective (Fig. S2 B). Moreover, the secretion of a subset of glycoproteins was also selectively blocked, similar to that in the *cdc20-1* mutant (Fig. S2, C and D). The observed secretion block after 3 h of nocodazole treatment is unlikely to be a direct effect of microtubule disruption on exocytosis in yeast. Brief treatment of the cells with nocodazole, though sufficient to disrupt microtubules, does not cause any detectable secretion block (unpublished data). The secretion effect after 3 h of nocodazole treatment is probably caused by mitotic arrest of the cells as a result of microtubule disruption (Quinlan et al., 1980; Holm et al., 1985).

As the function of Cdc20 and APC complex is ultimately linked to Cdk1, we hypothesize that the defect in exocytosis observed in metaphase-arrested cells is caused by elevated Cdk1 activity. We reasoned that if Cdk1 activity were inhibited in the *cdc20-1* cells, then Bgl2 secretion would be restored. To test this prediction, we assayed Bgl2 secretion in *cdc20-1* cells that contain an analogue-sensitive *cdk1* allele (*cdk1-as*), which encodes a mutant kinase that can be specifically inhibited by 1NM-PP1 (Bishop et al., 2000). We arrested *cdc20-1 cdk1-as* double mutant cells in metaphase by shifting them to 37°C for 90 min and then added 1NM-PP1 to inhibit Cdk1. Within 30 min of 1NM-PP1 treatment, the intracellular fraction of Bgl2 decreased significantly compared with mock-treated cells (Fig. 2, A and B). We also examined vesicle accumulation in *cdc20-1* and *cdc20-1 cdk1-as* cells with INM-PP1 treatment after they were arrested at metaphase using thin-section EM. As shown in Fig. 2 (C and D), although there was an accumulation of vesicles (106 ± 35 vesicles per section) in the *cdc20-1* cells, there were many fewer vesicles (<10 vesicles per section) in the *cdc20-1 cdk1-as* cells after 1NM-PP1 treatment. These data suggest that mitotic Cdk1 activity mediates the block in exocytosis during metaphase. Alternatively, but not mutually exclusively, it is possible that Cdk1 inhibition alleviated the secretion defect by allowing the *cdc20* cells to exit M phase. In either case, the data demonstrate that exocytosis is negatively affected in mitotic arrested cells.

Exo84 is phosphorylated by mitotic Cdk1

How is exocytosis controlled during metaphase? When associated with the mitotic cyclins, Cdk1 controls the mitotic events in the cell cycle through phosphorylation (Mendenhall and Hodge, 1998). Through sequence analyses, we found that the exocyst

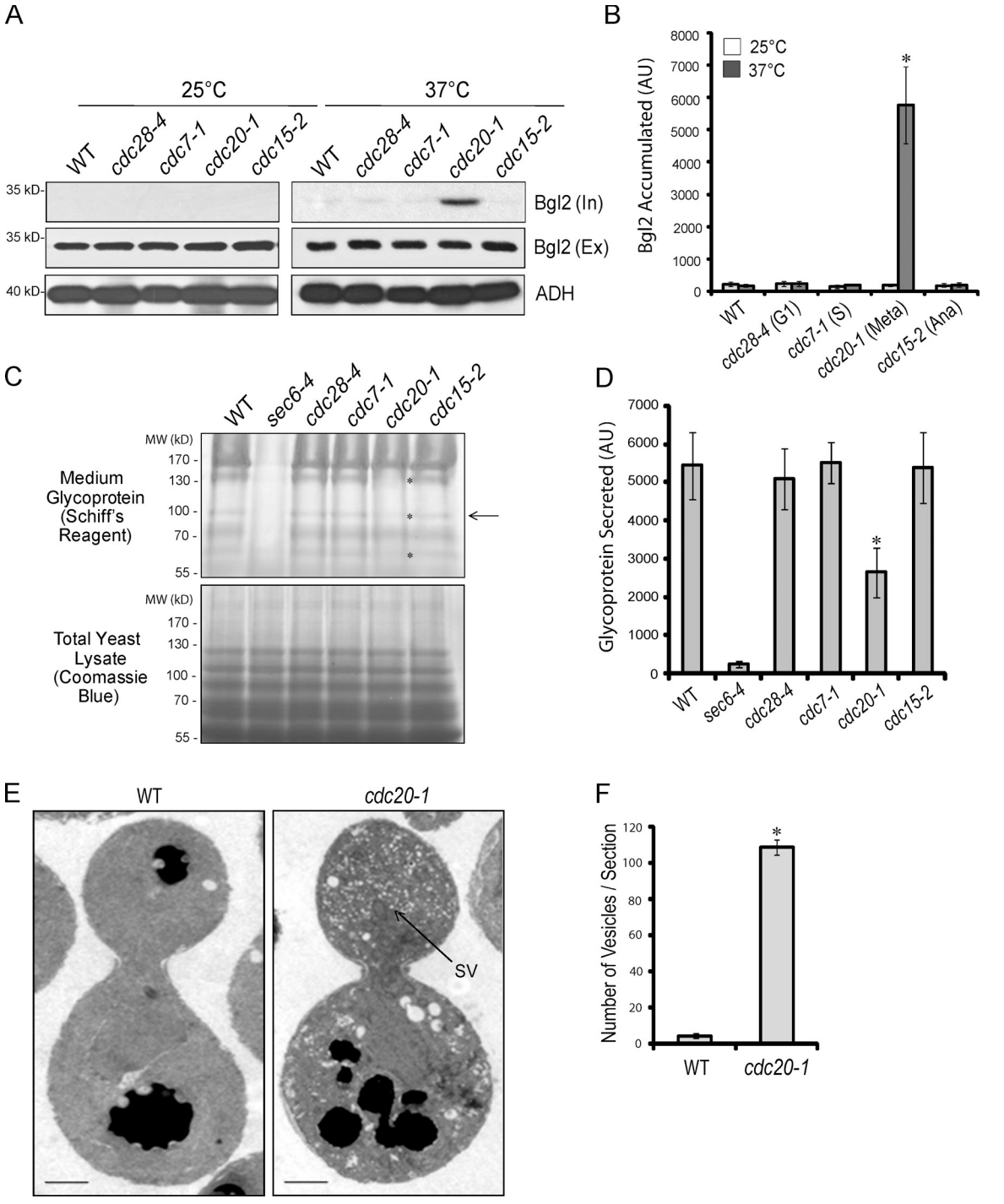

Figure 1. **Exocytosis is inhibited before metaphase-anaphase transition.** (A) The *cdc20-1* mutant exhibits Bgl2 secretion defects at the restrictive temperature. Cells were grown at 25°C or shifted to 37°C for 1.5 h. Internal (In) and external (Ex) pools of Bgl2 in wild-type, *cdc28-4* (G1 phase), *cdc7-1* (S phase), *cdc20-1* (metaphase), and *cdc15-2* (anaphase) cells were examined by Western blot analysis. Alcohol dehydrogenase (ADH) levels were probed as a protein loading control. (B) The internal accumulation of Bgl2 was quantified for the conditional cell cycle mutants. The stages of cell cycle arrest for these cells are indicated: Meta, metaphase; Ana, anaphase. AU, arbitrary units. Error bars represent standard deviation ($n = 3$). *, $P < 0.01$. (C) Selective block of glycoprotein secretion in the *cdc20-1* mutant at the restrictive temperature. The asterisks indicate the bands with reduced levels of secretion in the *cdc20-1* mutant. (D) Quantification of the levels of protein indicated by the arrow in C. Error bars represent standard deviation ($n = 3$). *, $P < 0.01$. (E) Thin-section EM shows that *cdc20-1* cells accumulate post-Golgi secretory vesicles (typically 80-100 nm in diameter) at the restrictive temperature. "SV" and the arrow indicate one of the vesicles. Bars, 1 µm. (F) Quantification of vesicle numbers per EM section detected in the wild-type and *cdc20-1* cells. Error bars represent standard error of the mean ($n = 35$). *, $P < 0.01$.

subunit Exo84 contains several consensus sites (*S/T-P-X-R/K; the asterisk indicates the phosphorylated serine or threonine residue) for Cdk1 phosphorylation. Furthermore, genome-scale phosphorylation studies show that Exo84 is phosphorylated by Cdk1 in vitro (Ubersax et al., 2003; Loog and Morgan, 2005; Kõivomägi et al., 2011). To determine if Exo84 is phosphorylated

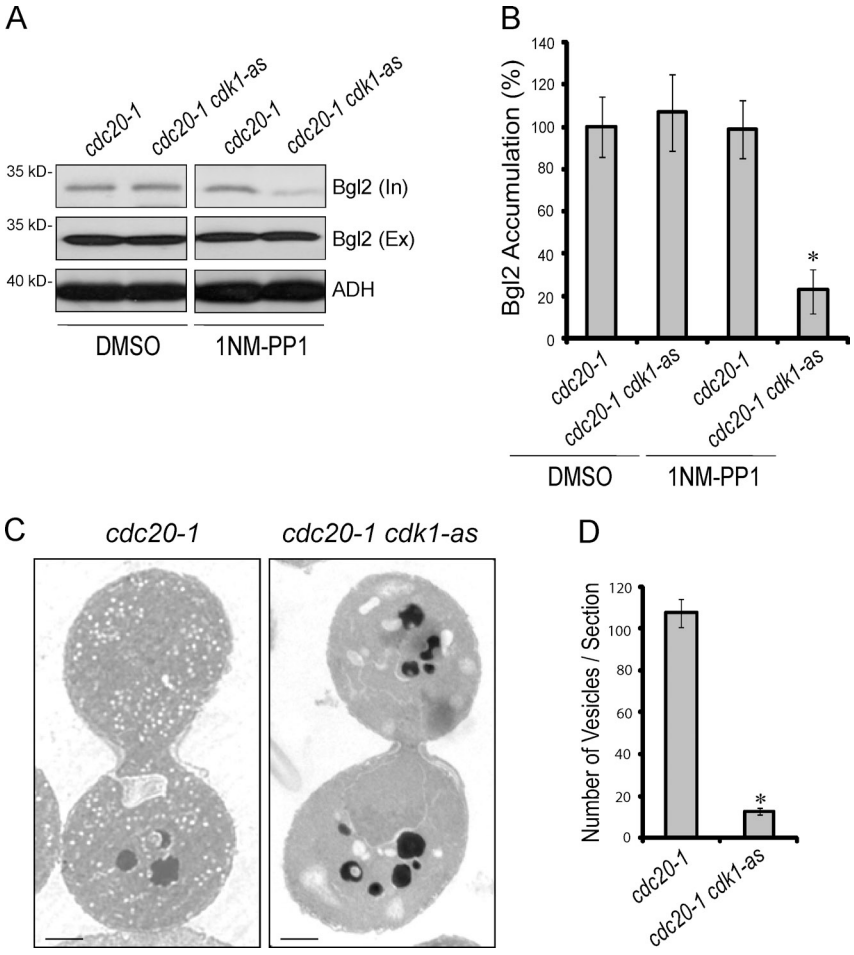

Figure 2. **Cdk1 activity is required for the secretion block in metaphase-arrested *cdc20-1* cells.** (A) The Bgl2 secretion block in *cdc20-1* cells depends on Cdk1 activity. *cdc20-1* and *cdc20-1 cdk1-as* cells were grown to early log phase at 25°C and shifted to 37°C for 1.5 h. Cells were then treated with DMSO (mock) or 15 µM 1NM-PP1 for 30 min. Internal and external pools of Bgl2 in *cdc20-1* and *cdc20-1 cdk1-as* cells were examined by Western blotting. ADH served as a protein loading control. (B) The accumulation of internal Bgl2 was quantified in each group, with the accumulation in *cdc20-1* cell treated with DMSO as 100%. Error bars represent standard deviation ($n = 3$). *, $P < 0.01$. (C) The *cdc20-1* and *cdc20-1 cdk1-as* cells were grown to early log phase at 25°C and shifted to 37°C for 1.5 h. Cells were then treated with 15 µM 1NM-PP1 for 30 min and proceeded for thin-section EM. The *cdc20-1* cells accumulated post-Golgi secretory vesicles at the restrictive temperature, whereas *cdc20-1 cdk1-as* did not. Bars, 1 µm. (D) Quantification of vesicle numbers per EM section in the *cdc20-1* and *cdc20-1 cdk1-as* cells. Error bars represent standard error of the mean ($n = 35$). *, $P < 0.01$.

by Cdk1 in cells, we immunoisolated Exo84 from yeast lysates and probed for Cdk1 phosphorylation using an antibody specific for Cdk1-phosphorylated peptides. As shown in Fig. 3 A, Exo84 was detected by the anti–phospho-substrate antibody, and the immunoreactivity was abolished by λ-phosphatase treatment. To verify the role of Cdk1 in Exo84 phosphorylation, we performed parallel experiment with the *cdk1-as1* cells. Although Exo84 phosphorylation was detected from mock-treated cells (DMSO), it was barely detectable from cells treated with 1NM-PP1.

Next, we examined Exo84 phosphorylation in synchronized cells. Yeast cells were first synchronized by α-factor treatment. The cells were then released from the arrest and collected at 15-min intervals. To detect Exo84 phosphorylation, Exo84 was immunoisolated from the cell lysates and run on the "Phos-Tag" protein gels, which specifically decrease the electrophoretic mobility of phosphorylated proteins for better separation from the nonphosphorylated population (Kinoshita et al., 2009). As shown in Fig. 3 B, Exo84 phosphorylation, as detected by decreased electrophoretic mobility, peaked around 100 min. This profile correlated with the expression of the B-type cyclin Clb2, a marker for M phase. In contrast, Cdc24, which is phosphorylated during G1/S phase (McCusker et al., 2007; Wai et al., 2009), displayed peak phosphorylation at 75 min. As an additional approach to study the cell cycle–dependent phosphorylation of Exo84, we probed immunoprecipitated Exo84 from cells arrested in G1 (with α-factor), S (with hydroxyurea), and M phase (with nocodazole) with the Cdk phospho-substrate antibody. As shown in Fig. 3 C, Exo84 is phosphorylated during M phase but not S phase. Exo84 phosphorylation also appeared slightly elevated in G1-arrested cells.

Because secretion is inhibited in *cdc20-1* cells arrested at metaphase, we checked whether Exo84 phosphorylation was also increased in this mutant. Immunoprecipitated Exo84 from the wild-type and *cdc20-1* cells grown at either 25°C or 37°C for 90 min, and the phosphorylation level of Exo84 was examined with the Cdk phospho-substrate antibody. As shown in Fig. 3 D, Exo84 phosphorylation significantly increased at 37°C compared with the wild-type cells.

To confirm that Exo84 is a direct substrate of mitotic Cdk1, GST-tagged Exo84 was expressed and purified from bacteria and incubated with Cln2–Cdk1, Clb5–Cdk1, or Clb2–Cdk1 in the presence of γ-[^{32}P]ATP. As shown in Fig. 3 E, Exo84 was phosphorylated by Clb2–Cdk1 but not Clb5–Cdk1, and to a lesser extent by Clb5–Cln2. As a control, GST was not phosphorylated by any Cdk1–cyclin complexes. We also mutated the five serine/threonine residues (T^{28}, S^{31}, S^{291}, S^{482}, and S^{716}) previously mapped by mass spectrometry to alanine (Smolka et al., 2007; Albuquerque et al., 2008; Holt et al., 2009). Clb2–Cdk phosphorylation of this mutant protein ("Exo84-A") was greatly diminished (Fig. 3 F).

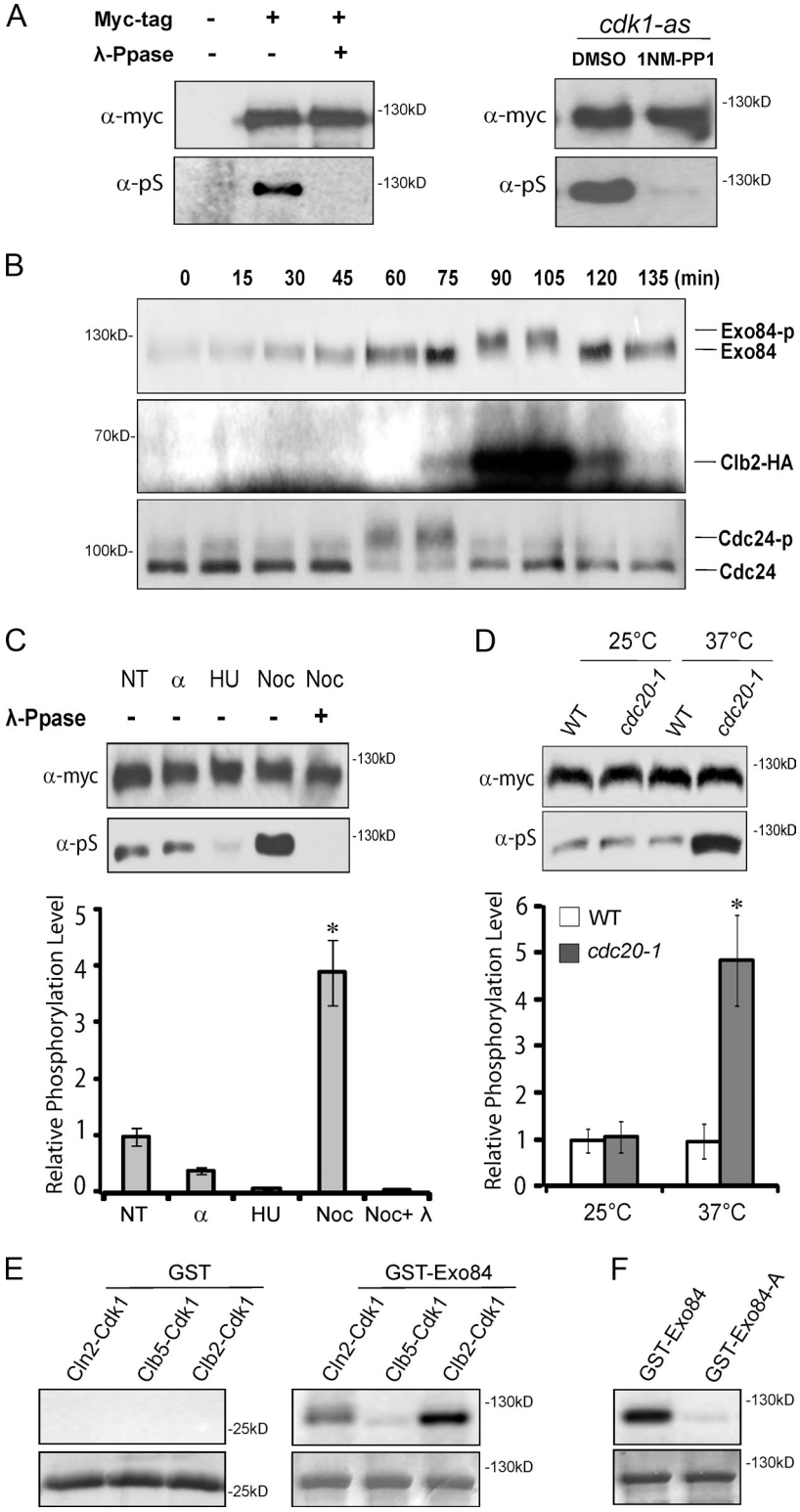

Figure 3. **Exo84 is phosphorylated by Cdk1 at M phase.** (A) Exo84 is phosphorylated in a Cdk1-dependent fashion in vivo. Cells expressing myc-tagged Exo84 (chromosomally integrated) were grown to early log phase at 25°C. Exo84-myc was immunoprecipitated and probed with anti-myc and anti–phospho-CDK substrate antibody (α-pS) by Western blotting. Untagged cells were used as a negative control. Where designated, immunoprecipitated Exo84 was treated with λ-phosphatase to abolish phosphorylation (left). Exo84 was immunoprecipitated from *cdk1-as* cells that were treated with DMSO (mock) or the Cdk1-as inhibitor 1NM-PP1 (right). Phosphorylation of Exo84 is reduced dramatically in *cdk1-as1* cells treated with 1NM-PP1. (B) Cell cycle–dependent phosphorylation of Exo84. Cells expressing Exo84-myc and Clb2-HA were synchronized at G1 with α-factor and then released and harvested at the indicated time points. The expression of Clb2-HA and the migration profiles of Exo84-myc and Cdc24 were examined by immunoblot analysis after the samples were separated on a Phos-tag PAGE gel that specifically retards the migration of phosphoproteins (see Materials and methods). (C) Exo84-myc was immunoprecipitated from asynchronous and cell cycle–arrested cells and then probed for Cdk1 phosphorylation by immunoblotting as in A. Where designated, samples were treated with λ-phosphatase (λ-Ppase). Wild-type cells were arrested in G1 phase with α-factor (α), S phase with hydroxyurea (HU), or M phase with nocodazole (Noc). Asynchronous cells are designated as "NT." Immunoblots reveal that Exo84 is heavily phosphorylated in M phase–arrested cells. Error bars represent standard deviation (n = 3). *, $P < 0.01$. (D) Exo84-myc was immunoprecipitated from the wild-type and *cdc20-1* mutant cells at the permissive or restrictive temperature, and then probed for Cdk1 phosphorylation by immunoblotting as in A. Error bars represent standard deviation (n = 3). *, $P < 0.01$. (E) Exo84 is phosphorylated by Cdk1 in vitro. GST and GST-Exo84 were purified from *Escherichia coli* and incubated with Cln2–Cdk1, Clb5–Cdk1, or Clb2–Cdk1 in the presence of γ-[^{32}P]ATP. Exo84 phosphorylation was detected by autoradiography (top). Corresponding Coomassie blue–stained gels are shown on the bottom. (F) In vitro Clb2-Cdk1 kinase assays with recombinant Exo84-A, which lacks the five Cdk1 phosphorylation sites. The phosphorylation of Exo84-A by mitotic Clb2–Cdk1 is barely detectable.

Exo84 phosphorylation inhibits the assembly of the exocyst complex

How does Cdk1 phosphorylation of Exo84 inhibit exocytosis? Because the assembly of the exocyst complex mediates the tethering of post-Golgi secretory vesicles to the plasma membrane, one possible effect of mitotic Cdk1 phosphorylation is to affect the association of Exo84 with rest of the exocyst complex. Exo84 bound directly to Sec5 and Sec10, and can coimmunoprecipitate all the exocyst components (Guo et al., 1999). We mutated the five phosphorylation sites of Exo84 to alanine ("Exo84-A") or to glutamate ("Exo84-E") and expressed these mutants in *exo84Δ* cells under the control of an endogenous *EXO84* promoter. Western blotting confirmed that the expression of the mutant Exo84 was comparable to that of the wild-type

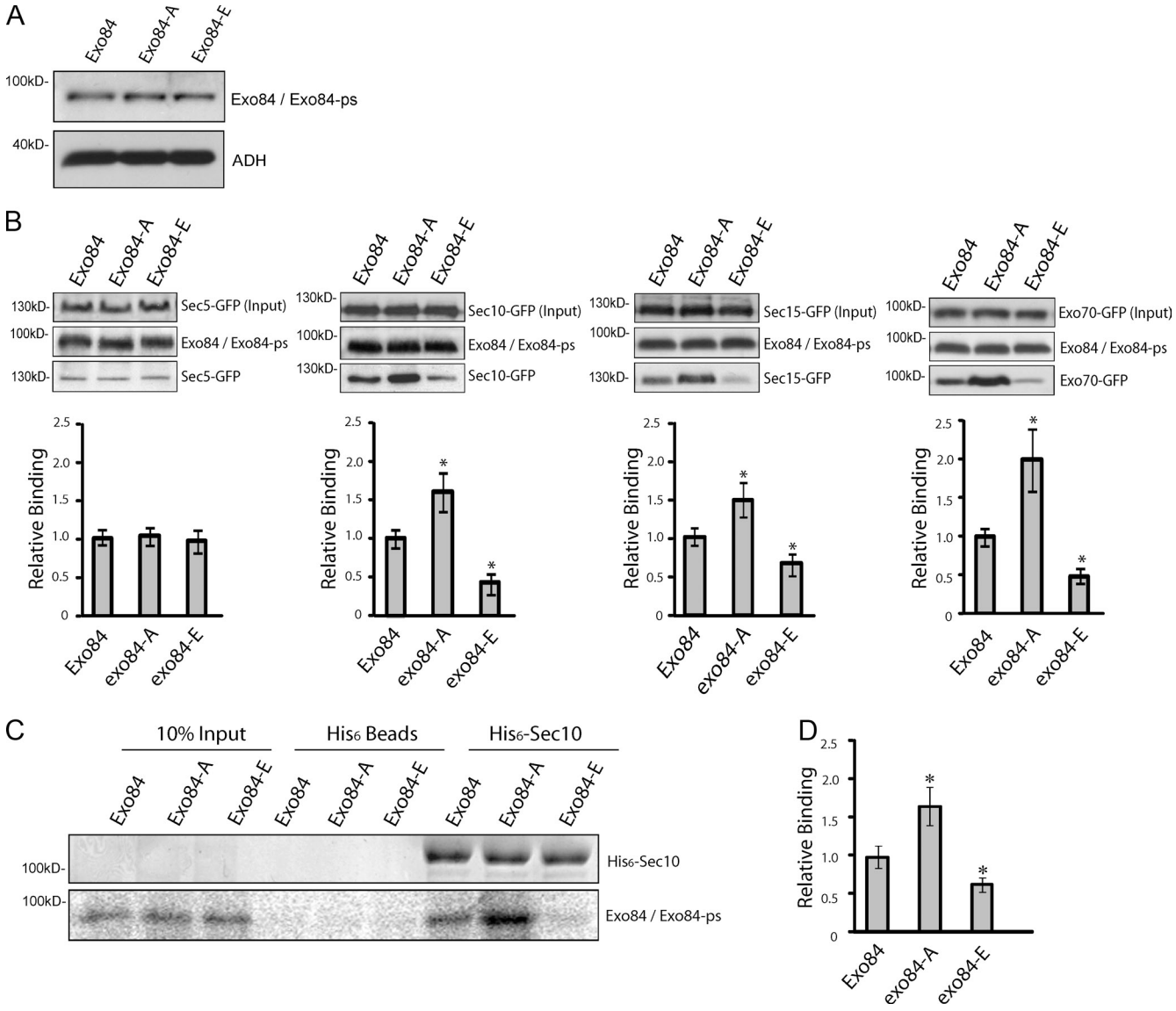

Figure 4. **Cdk1 phosphorylation inhibits the interaction of Exo84 with other exocyst components.** (A) Immunoblots of cells expressing wild-type and mutant Exo84 (Exo84-A and Exo84-E) proteins. Exo84 was detected using a rabbit anti-Exo84 antibody. ADH was probed as a protein loading control. (B) Exo84 phosphorylation negatively regulates exocyst assembly. Cells were grown to early log phase at 25°C. Then wild-type and mutant Exo84 were immunoprecipitated from cells coexpressing a GFP-tagged exocyst protein (Sec5, Sec10, Sec15, or Exo70, tagged by chromosomal integration). Co-immunoprecipitated exocyst proteins were probed with an anti-GFP antibody. The relative amounts of coprecipitated Sec10-GFP, Sec15-GFP, and Exo70-GFP were higher in the *exo84-A* mutant and lower in the *exo84-E* mutant. The amount of coimmunoprecipitated Sec5-GFP is similar for all Exo84 variants. The quantification of the binding is shown below each Western blot. Error bars represent standard deviation. *, $P < 0.01$; $n = 3$. (C) Phosphorylation negatively regulates Exo84 interaction with Sec10. Exo84, Exo84-A, and Exo84-E were synthesized by in vitro transcription/translation in the presence of [^{35}S]methionine/cysteine. The proteins were then incubated with purified recombinant His_6-tagged Sec10 conjugated to Ni-Sepharose. After extensive washing, the bound proteins were analyzed by SDS-PAGE and autoradiography. The Coomassie blue–stained gel (top) shows the inputs of His_6-tagged Sec10 protein. The autoradiograph (bottom) shows the input (10%) and bound [^{35}S]methionine-labeled Exo84 and Exo84 phospho mutants (Exo84-ps). The binding of His_6-Sec10 with Exo84 and *exo84* was quantified in D. Error bars represent standard deviation ($n = 3$). *, $P < 0.01$.

Exo84 (Fig. 4 A). Immunoprecipitation was performed using an anti-Exo84 antibody, and the amounts of associated exocyst components were examined by Western blotting. As shown in Fig. 4 B, the phosphomimetic Exo84-E mutant exhibited diminished interactions with Sec10, Sec15, and Exo70 compared with the wild-type Exo84. Conversely, the phospho-deficient Exo84-A protein exhibited enhanced interactions with Sec10, Sec15, and Exo70. Neither Exo84 mutant affected Sec5 binding. Because the coprecipitation of Exo84 with Sec10, but not Sec5, was affected, we predicted that the direct interaction between Sec10 and Exo84 would be altered by Cdk1 phosphorylation. We performed in vitro binding assays with recombinant His_6-Sec10 and in vitro translated ^{35}S-labeled Exo84. As shown in Fig. 4 (C and D), compared with the wild-type Exo84, Exo84-E binding to Sec10 was significantly reduced. Because Sec10 directly binds Sec15 and Exo70 (Guo et al., 1999; Dong et al., 2005), the diminished Exo84–Sec10 interaction observed with the phosphomimetic Exo84-E may account for the reduced Exo84 coimmunoprecipitation of Sec15 and Exo70 (Fig. 4 B).

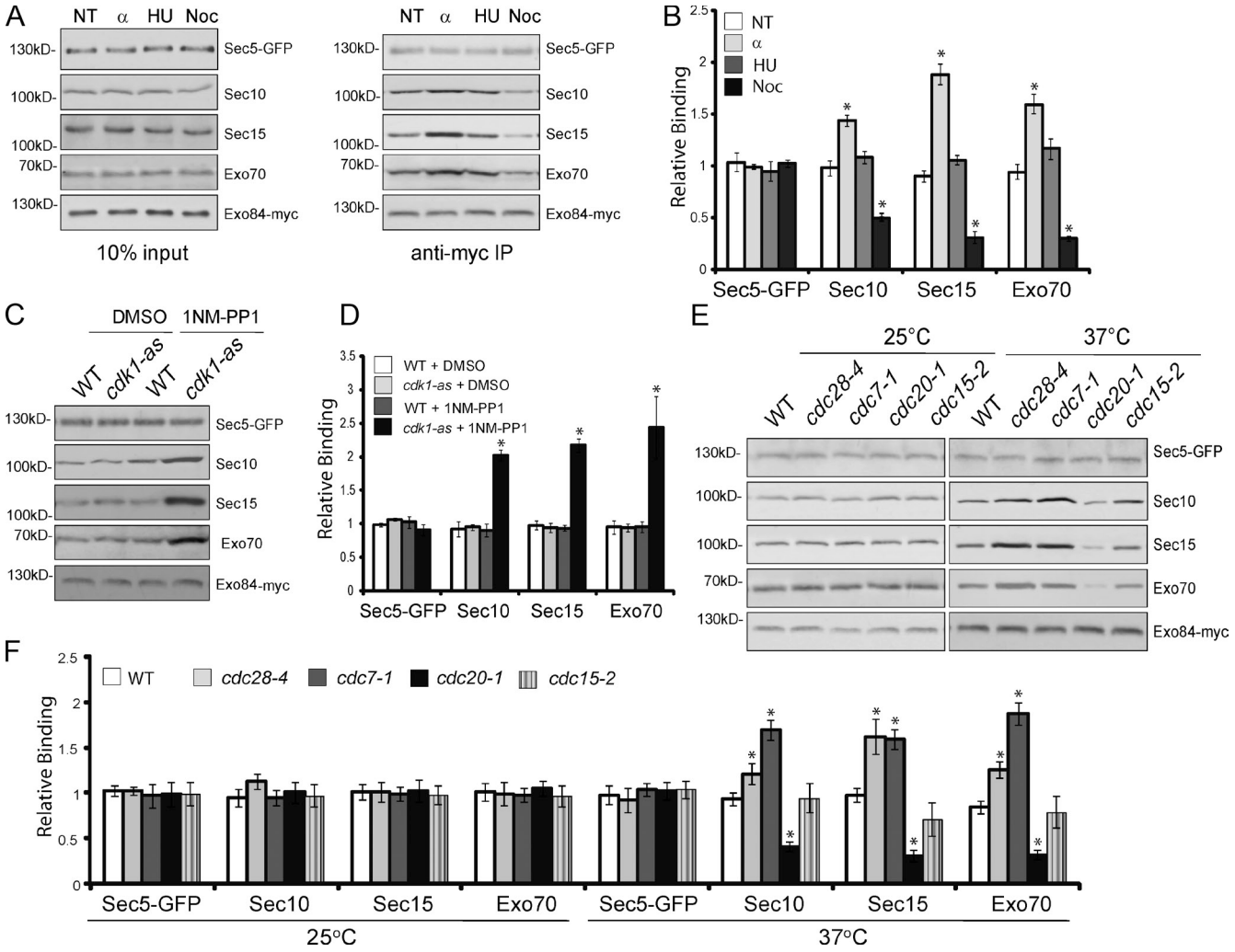

Figure 5. **The assembly of the exocyst complex is inhibited during M phase.** (A) Exo84 was tagged by the myc epitope by chromosomal integration. Cells expressing Exo84-myc were synchronized in G1, S, and M phase with α-factor (α), hydroxyurea (HU), and nocodazole (Noc), respectively. Exo84-myc was immunoprecipitated using the anti-myc antibody, and Western blots were performed to detect the amounts of coprecipitating Sec5-GFP, Sec10, Sec15, and Exo70. (left) The expression of the exocyst subunits cell extracts ("10% input"). (right) The amounts of the exocyst subunits coimmunoprecipitated with Exo84-myc. (B) Quantification of the amounts of the exocyst coimmunipreciptated with Exo84-myc. The levels of binding in different groups with respect to that of the nontreated (NT) cells ("relative binding") were shown. The levels of binding for Sec10, Sec15, and Exo70 decrease in the nocodazole-treated cells. Sec5 binding remains unchanged. Error bars represent standard deviation. *, $P < 0.01$; $n = 3$. (C) Inhibition of Cdk1 promotes exocyst assembly. The wild-type and *cdk1-as* cells were treated with DMSO (mock) or 1NM-PP1 before Exo84-myc coimmunoprecipitation. The levels of binding of Sec10, Sec15, and Exo70 increased in the *cdk1-as* cells treated with 1NM-PP1, whereas their binding with Sec5 remained unchanged. (D) Quantification of binding for C was performed as described in B. Error bars represent standard deviation. *, $P < 0.01$; $n = 3$. (E) The *cdc20-1* mutant exhibits exocyst assembly defects at the restrictive temperature. The wild-type and different cell cycle mutant cells were grown at 25°C and shifted to 37°C for 2 h. Exo84-myc immunoprecipitation was performed using these cells. The levels of binding of Sec10, Sec15, and Exo70 decreased in the *cdc20-1* mutant. (F) Quantification of the amounts of the exocyst coimmunipreciptated with Exo84-myc. The levels of binding for Sec10, Sec15, and Exo70 decreased in the *cdc20-1* mutant. Sec5 binding remains unchanged. Error bars represent standard deviation. *, $P < 0.01$; $n = 3$.

Exocyst assembly is inhibited during mitosis

To determine whether the assembly of the exocyst complex is inhibited in M phase, in which the Cdk1-Clb2 is most active, we immunoprecipitated Exo84 from yeast cells arrested at G1 (treated with α-factor), S (treated with hydroxyurea), and M (treated with nocodazole) phases and probed for associated exocyst components by Western blotting. As shown in Fig. 5 (A and B), Exo84 bound less to Sec10, Sec15, and Exo70 in M phase–arrested cells than those in G1 or S phase–arrested cells, whereas Sec5 binding was unchanged. These data suggest that exocyst assembly is blocked during metaphase. We also performed the immunoprecipitation experiment using the analogue-sensitive *cdk1* cells. As shown in Fig. 5 (C and D), treatment of the *cdk1-as* cells with 1NM-PP1 for 30 min led to an increase of Exo84 binding to Sec10, Sec15, and Exo70, but not for Sec5-GFP. As controls, the wild-type or mock-treated *cdk1-as* cells did not show such an effect. Collectively, the data further suggest that Cdk1 phosphorylation blocks the exocyst assembly.

To test the exocyst assembly in *cdc* mutants arrested at different stages of the cell cycle, Exo84 was immunoprecipitated from the wild-type and *cdc* mutants grown either at 25°C or shifted to 37°C for 1.5 h. As shown in Fig. 5 (E and F), although Sec5 binding was unchanged, the binding of Sec10,

Sec15, and Exo70 to Exo84 decreased in the *cdc20-1* mutant cells compared with the wild-type or other *cdc* mutants at the restrictive temperature, which suggests that exocyst assembly is inhibited at metaphase. We also noticed that the binding of Sec10, Sec15, and Exo70 to Exo84 increased in the *cdc28-4* and *cdc7-1* mutants. We will follow up on this interesting observation in future studies.

In addition to *cdc* mutants, we have also examined exocyst assembly in cells arrested to metaphase by nocodazole treatment. Comparing to the nontreated cells, the *cdk1-as* cells treated with nocodazole for 3 h showed an increased level of Exo84 phosphorylation (Fig. S3 A) and a decreased level of exocyst assembly (Fig. S3 B). Further addition of 1NM-PP1, however, reduced Exo84 phosphorylation and alleviated the exocyst assembly defect. These data are consistent with the results obtained using the *cdc20-1* mutant.

Exo84 phosphorylation inhibits exocytosis and cell growth

To determine the physiological consequence of Exo84 phosphorylation, we examined the secretion properties of the *exo84* mutant cells. Although there was no block of Bgl2 secretion in the wild-type and *exo84-A* cells, the *exo84-E* cells displayed intracellular accumulation of Bgl2 (Fig. 6, A and B). In addition, thin-section EM analyses showed an accumulation of 80–100-nm-diameter secretory vesicles in the *exo84-E* cells (Fig. 6, C and D). To more closely examine the effect *exo84-A* on secretion, we generated double mutant strains in which the two Exo84 phospho mutants were expressed in the *exo70-38* mutant background. As shown in Fig. 6 (E and F), the *exo70-38* single mutant cells ("*exo70-38 EXO84*") exhibited a Bgl2 secretion block, and the *exo70-38 exo84-E* double mutant cells displayed an even more pronounced Bgl2 secretion defect. Interestingly, the Bgl2 secretion defect was significantly reduced in the *exo70-38 exo84-A* double mutant cells compared with the *exo70-38* single mutant, which indicates that the expression of the phosphorylation-deficient Exo84-A mutant has a rescuing effect on the *exo70-38*. These phenotypes were also confirmed by thin-section EM, as there were more vesicles accumulated in the *exo70-38 exo84-E* double mutant cells, and fewer vesicles in the *exo70-38 exo84-A* double mutant cells (Fig. 6, G and H).

The growth properties of the Exo84 mutant cells correlate with the observed secretion properties. The *exo84-E* mutant grew slower than the wild-type cells, whereas the *exo84-A* mutant grows slightly faster than wild-type *EXO84* cells. Moreover, the *exo70-38 exo84-E* double mutant cells grew more poorly than the *exo70-38* single mutant cells, and the *exo70-38 exo84-A* double mutant cells showed much improved growth (Fig. 6 I). In addition to *exo70-38*, the *exo84* phospho mutants had similar synthetic effects when combined with other exocyst mutants (unpublished data). The use of double mutants allowed us to study the positive effect of *exo84-A* on exocytosis. To directly examine the effect of the *exo84-A* mutant on exocytosis, we compared media glycoprotein secretion by the wild-type and *exo84-A* mutant cells released from α-factor arrest at 30 and 90 min, respectively. At 90 min (corresponding to metaphase), the secretion of a select set of glycoproteins was lower than that at 30 min (G1 phase; Fig. 7). This correlates with the phosphorylation of Exo84 around 90 min (Fig. 3 B). However, the secretion of the *exo84-A* mutant cell was the same for both 30 min and 90 min. Together, our data suggest that Exo84 phosphorylation plays a negative regulatory role on exocytosis.

Exo84 phosphorylation regulates daughter cell growth during mitosis

During M phase, yeast growth is restricted to the daughter cell (the "bud"), whereas the mother cell remains largely unchanged. Given that Exo84 phosphorylation inhibits exocytosis in the M phase, we predicted that bud growth would be affected by Exo84 phospho mutants. To test this prediction, we examined bud growth in wild-type, *exo84-A*, and *exo84-E* mutant cells by time-lapse microscopy. We determined the cell cycle phases by surveying nuclear position and morphology using a MARS-tagged nuclear envelope protein (Nup57-MARS) as described previously (Khmelinskii et al., 2010). We also monitor GFP-tagged Sec5, which relocates to the mother–daughter junction to mediate abscission at the end of mitosis. Sec5 was chosen because it is not affected by Exo84 phosphorylation (see Fig. 4 B). As expected, we observed that the size of mother cells remain similar in wild-type and *exo84* phosphorylation mutants. In contrast, the buds of mitotic *exo84-A* cells typically grew larger than the buds of corresponding wild-type cells. Moreover, the buds of mitotic *exo84-E* cells were smaller than those of wild-type and *exo84-A* cells (Fig. 8 A and Fig. S4). As a result, upon completion of mitosis and cytokinesis, the daughter cells were smaller for *exo84-E* and larger for *exo84-A* cells. A comparison of the sizes, presented as the daughter/mother size ratios, is shown in Fig. 8 B. The data suggest that Cdk1 phosphorylation of Exo84 controls cell growth homeostasis.

Discussion

Regulation of cell growth and surface expansion is a basic feature of cell cycle progression. Over the past decades, while several aspects of cell cycle such as DNA replication and chromosomal segregation have been intensively studied, the molecular mechanisms that control cell membrane growth remain unknown (Jorgensen and Tyers, 2004; Goranov and Amon, 2010). A conspicuous feature of the M-phase cells is the reduction of surface growth, which helps the cells to adapt to the energy demands and reorganize cellular structures for chromosomes segregation and organelle inheritance (Mitchison and Nurse, 1985; Lucocq and Warren, 1987; Kreiner and Moore, 1990; Leaf et al., 1990; Lowe et al., 1998; Seemann et al., 2002; Boucrot and Kirchhausen, 2007, 2008; Peng and Weisman, 2008; Goranov et al., 2009; Tzur et al., 2009; Goranov and Amon, 2010). Membrane growth relies on the tight control of exocytosis, by which proteins and lipids are incorporated into the plasma membrane. A recent microscopic study elegantly demonstrated that mammalian cells undergo up to several folds of surface area reduction during M phase followed by a compensatory increase in surface area from anaphase to cytokinesis, and expression of dominant-negative v-SNARE proteins (Vamp3 and Vamp7) that mediate vesicle fusion at the plasma membrane blocks growth recovery during anaphase (Boucrot and Kirchhausen, 2007).

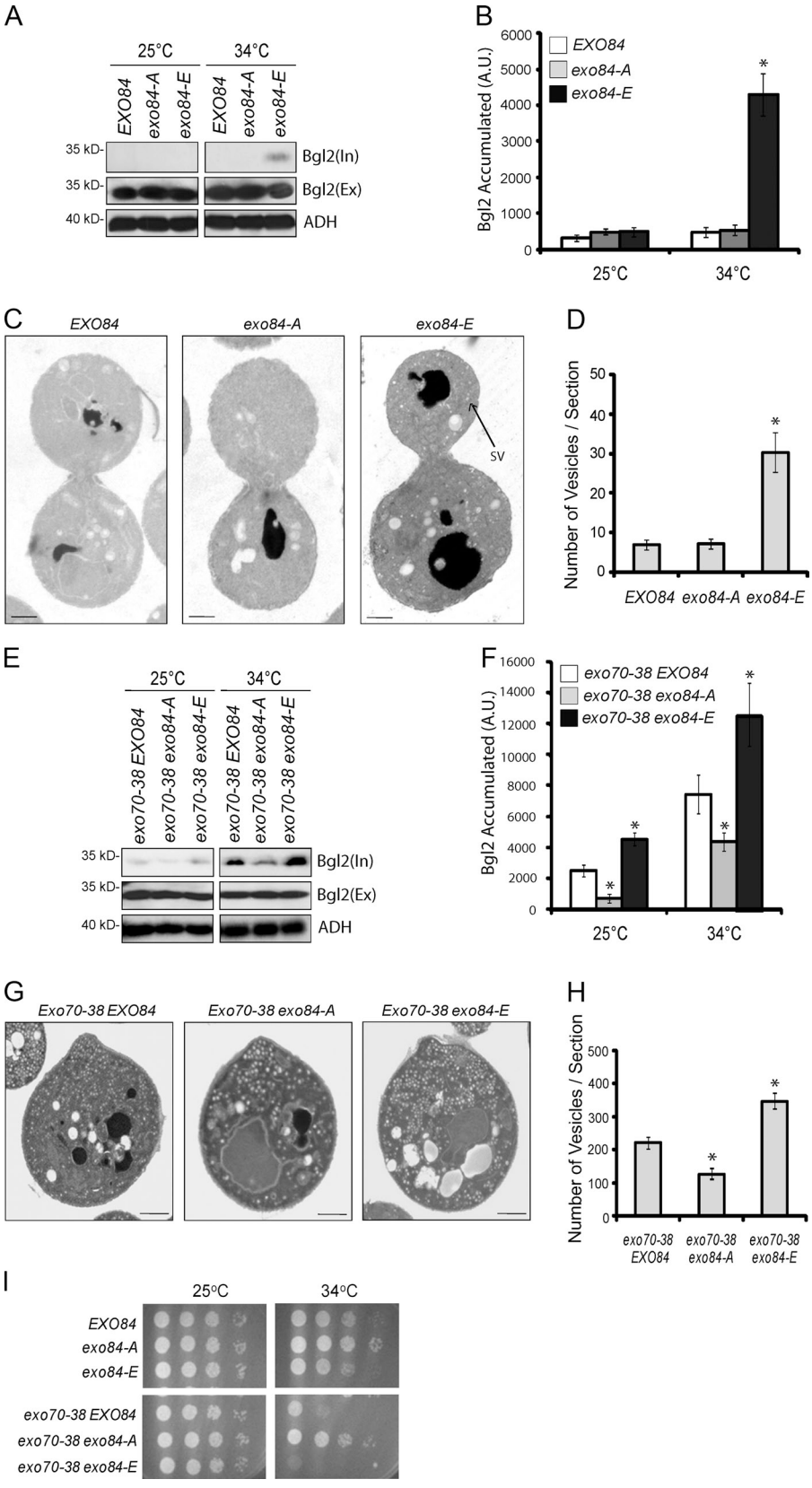

Figure 6. **Exo84 phosphorylation inhibits exocytosis.** (A) Bgl2 secretion assays in the wild-type (*EXO84*), *exo84-A*, and *exo84-E* cells at 25°C and 34°C. The *exo84-E* mutant accumulates Bgl2 in the cell at 34°C. (B) Quantification of Bgl2 accumulation in the wild-type, *exo84-A*, and *exo84-E* cells at 25°C and 34°C. Error bars represent standard deviation. *, $P < 0.01$; $n = 3$. (C) Thin-section EM analysis of the wild-type, *exo84-A*, and *exo84-E* cells after shifted to 34°C for 90 min. "SV" and the arrow indicate one of the vesicles. Bars, 1 µm. (D) Quantification of accumulated vesicles in the wild-type, *exo84-A*, and *exo84-E* cells. Error bars represent standard error of the mean ($n = 35$). *, $P < 0.01$. (E) Exo84 phosphorylation site mutations affect Bgl2 secretion in the *exo70-38* mutant background. The *exo70 exo84* double mutants were generated and assayed as outlined in A. The *exo70-38 exo84-E* cells displayed more pronounced Bgl2 secretion defects than corresponding *exo70-38* single mutant cells, whereas the *exo70-38 exo84-A* cells displayed diminished Bgl2 secretion defects compared with the *exo70-38* single mutant cells. (F) Quantification of Bgl2 accumulation in the *exo70-38 EXO84*, *exo70-38 exo84-A*, and *exo70-38 exo84-E* mutant cells. Error bars indicate standard deviation. *, $P < 0.01$; $n = 3$. (G) Thin-section EM analysis of the *exo70 exo84* double mutant cells. The *exo70-38 exo84-A* cells contain fewer secretory vesicles than *exo70-38* single mutant cells, whereas *exo70-38 exo84-E* cells accumulate a larger number of secretory vesicles than *exo70-38* cells. Bars, 1 µm. (H) Quantification of accumulated vesicles in the *exo70-38 EXO84*, *exo70-38 exo84-A*, and *exo70-38 exo84-E* mutant cells. Error bars represent standard error of the mean. *, $P < 0.01$; $n = 35$. (I) Growth of the wild-type (*EXO84*), *exo84-A*, *exo84-E*, *exo70-38*, *exo70-38 exo84-A*, and *exo70-38 exo84-E* cells after serial dilution on plates at 25°C and 34°C. The *exo84-E* cells grew poorly at 34°C compared with the wild-type and *exo84-A* cells. The *exo70-38 exo84-A* cells grew better than the *exo70-38* single mutant, whereas *exo70-38 exo84-E* cells displayed severe growth defects at 34°C.

The budding yeast *S. cerevisiae* has been used as an invaluable model system in the study of both cell cycle regulation and membrane trafficking. Over the years, the generation and characterization of a wealth of cell division cycle mutants ("*cdc*") and secretion mutants ("*sec*") have significantly contributed to the understanding of the fundamental mechanisms of cell cycle and membrane trafficking in eukaryotic cells. More recently, cell growth and morphogenesis have also been

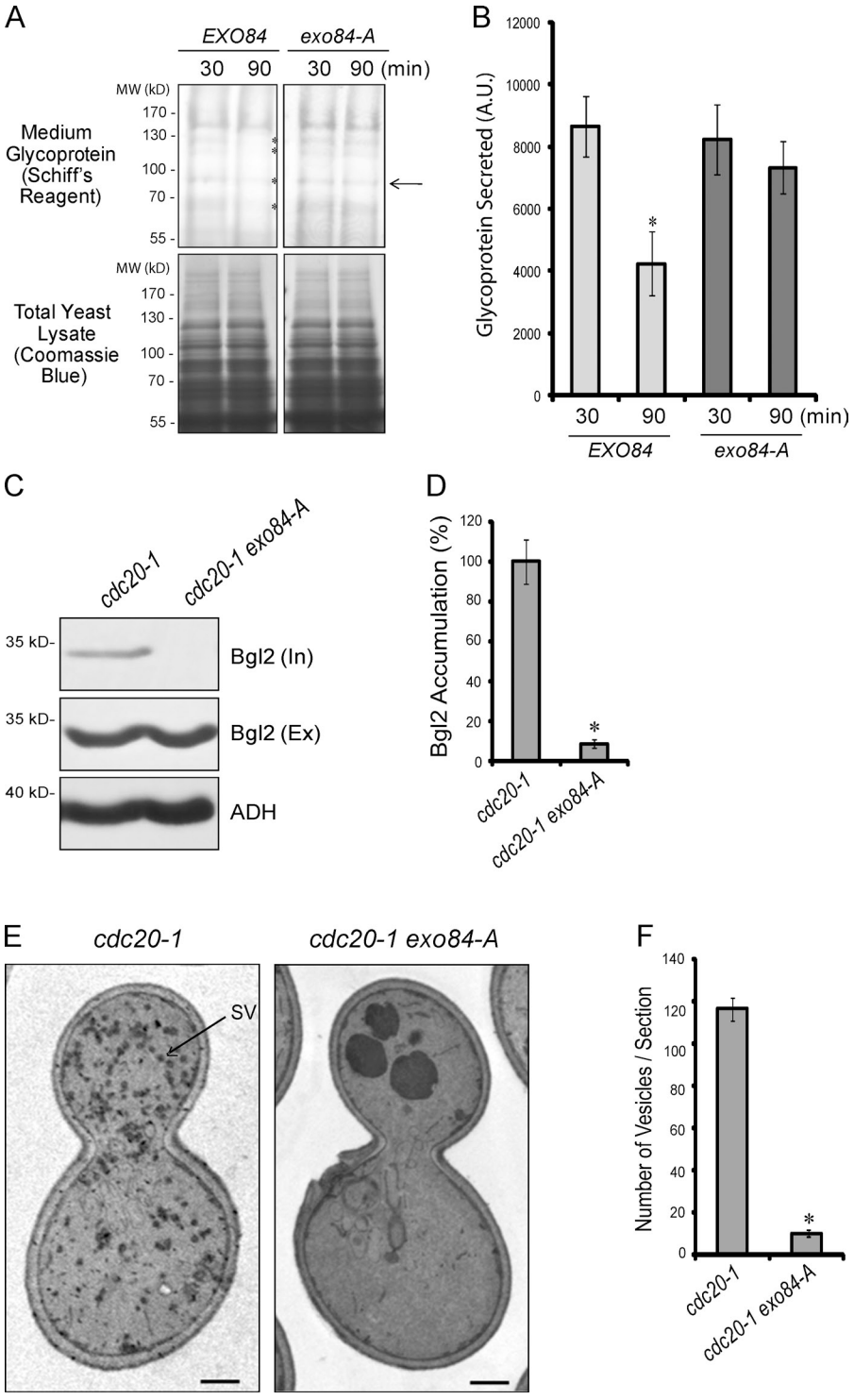

Figure 7. **Exo84 phosphorylation is required for secretion block at metaphase.** (A) Glycoprotein secretion defects in cells during metaphase. The wild-type and *exo84-A* cells were synchronized with α-factor and then released for 30 min (approximately interphase stage) and 90 min (approximately metaphase stage), respectively. These are the two time points at which electrophoretic mobility (i.e., phosphorylation state) of Exo84p is significantly distinct from each other according to Fig. 3 B. The media glycoproteins were collected and analyzed. Asterisks indicate the glycoproteins that were changed comparing the wild-type and *exo84-A* strains. Protein molecular weights are indicated to the left (kD). (B) Quantification of the glycoprotein band indicated by the arrow in A. Error bars represent standard deviation. *, $P < 0.01$; $n = 3$. (C) The phospho-deficient *exo84-A* mutant rescued the Bgl2 secretion defect of the *cdc20-1* cells. The *cdc20-1* and *cdc20-1 exo84-A* mutants were grown at 25°C and then shifted to 37°C for 1.5 h. Internal (In) and external (Ex) pools of Bgl2 were examined by Western blot analysis. ADH was probed as a protein loading control. (D) Quantification of Bgl2 accumulation in the *cdc20-1* and *cdc20-1 exo84-A* mutants at 37°C. Error bars represent standard deviation. *, $P < 0.01$; $n = 3$. (E) Cells were fixed with permanganate and processed for thin-section EM. The *cdc20-1* cells accumulated post-Golgi secretory vesicles at the restrictive temperature, whereas *cdc20-1 exo84-A* double mutant did not. "SV" and the arrow indicate one of the vesicles. Bars, 1 µm. (F) Quantification of accumulated vesicles in the *cdc20-1* and *cdc20-1 exo84-A* mutants at 37°C. Error bars represent standard error of the mean. *, $P < 0.01$; $n = 35$.

carefully investigated in each cell cycle stage in the budding yeast (Goranov and Amon, 2010; McCusker and Kellogg, 2012). Compelling evidence has shown the coordination of cell cycle with membrane growth (McCusker et al., 2007; Goranov et al., 2009). Here, using secretion assays, we demonstrate that exocytosis is inhibited in yeast cells defective in the metaphase–anaphase transition. Furthermore, thin-section EM revealed that the metaphase mutant cells accumulate 80–100-nm-diameter vesicles, which is a well-established feature of the post-Golgi secretion mutants (Novick et al., 1980). This is the first time *cdc* mutants (*cdc20-1* and *cdc23-1*) are found to have defects similar to the post-Golgi *sec* mutants such as those for the exocyst subunits. Further analyses using the analogue-sensitive *cdc28* mutant (*cdk1-as*) suggest that elevated Cdk1 kinase activity during the M phase is the primary cause for the exocytosis block in the *cdc* mutant. Interestingly, we found that the secretion of a select set of cargo proteins was blocked. Unlike Bgl2, no defect was detected for

invertase secretion. Previous studies have demonstrated that invertase represents only one branch of the exocytic routes in yeast (Harsay and Bretscher, 1995; Harsay and Schekman, 2002). It was also shown that, in *cdc42* and *exo70* (a component of the exocyst complex) mutants, although Bgl2 secretion was blocked and the cells clearly accumulated secretory vesicles as shown by EM, invertase secretion was not affected in these cells (Adamo et al., 2001; He et al., 2007). Similarly, analysis of glycoproteins secreted in the media also revealed the block of a subset of proteins in metaphase-arrested cells. Note that these glycoproteins are only the soluble proteins in the media. This assay does not allow the analysis of the transmembrane proteins incorporated into the plasma membrane via exocytosis. Future studies are needed to investigate why specific exocytosis routes are affected in mutants blocked at the metaphase.

In addition to using *cdc* mutants, we also investigated secretion in cells treated with nocodazole, which disrupts microtubules and affects chromosomal segregation, thus arresting cells at the metaphase (Quinlan et al., 1980; Holm et al., 1985). We observed secretion defects of a select subset of proteins in these cells similar to those of the *cdc20-1* cells. Note that, in our experiments, cells were treated with nocodazole for 3 h, which is commonly used in the field to synchronize cells to metaphase (a long period of treatment time is usually needed, as the cell cycle still progresses until reaching metaphase; Quinlan et al., 1980; Holm et al., 1985). It is unlikely that microtubule disruption directly affects exocytosis in the budding yeast; a brief treatment of the cells with nocodazole, though sufficient to disrupt microtubules, does not cause any detectable secretion block (unpublished data).

In the wild-type yeast cells, the metaphase–anaphase transition takes place very transiently (Shaw et al., 1998). As such, the cells do not accumulate significant amounts of cargos that are readily detectable with methods such as the Bgl2 assay (Adamo et al., 2001). With a total media glycoprotein assay, we were able to detect secretion block for a subset of cargos in the wild-type cells synchronized to metaphase compared with cells at G1 phase (Fig. 7, A and B). The *cdc* mutants and nocodazole treatment allow the arrest of the cell cycle, which provides enough time for vesicle accumulation that allows a clear detection of the secretion block. It is not clear why a select set of proteins is affected. It will be interesting to investigate the relationship of the subset of cargos and the specific exocytic route with growth arrest at metaphase.

At the molecular level, we demonstrate that the exocyst is a direct target of mitotic Cdk1. Our data show that Cdk1-mediated phosphorylation of Exo84 inhibits the assembly of the exocyst complex, thereby preventing secretory vesicle docking to the plasma membrane for exocytosis and cell surface expansion. Blocking Exo84 phosphorylation enhanced exocytosis and led to increased bud growth during M phase. In contrast, the phospho-mimicry *exo84* mutant has smaller daughter cells upon completion of mitosis. Our study demonstrates the coordination between membrane trafficking and cell cycle progression, and provides a molecular mechanism for cell growth inhibition during metaphase.

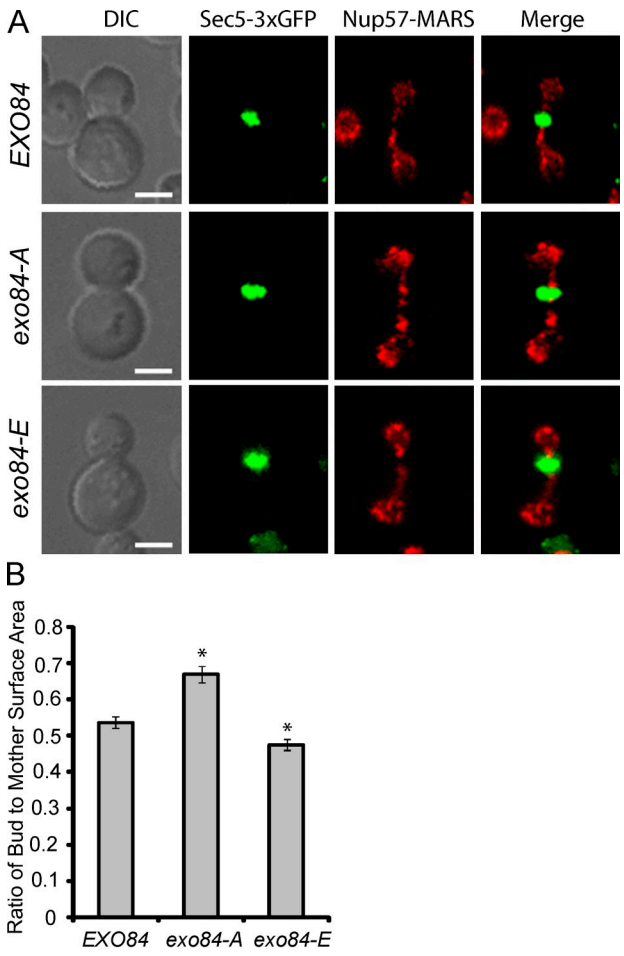

Figure 8. **Exo84 phosphorylation inhibits daughter cell surface expansion.** (A) The growth of the wild-type and *exo84* phosphorylation mutants coexpressing Sec5-3×GFP and Nup57-MARS (a nuclear envelope marker) was monitored by time-lapse microscopy (see Fig. S4 for the time-lapse images). Representative images of cells at the end of mitosis as indicated by relocalization of Sec5-3×GFP to the bud neck are shown. Anaphase and metaphase phase were determined by nuclear morphology using Nup57-MARS as a marker. DIC, differential interference contrast. Bars, 2.5 µm. (B) The ratios of daughter cell ("bud") to mother cell surface areas at late mitotic phase were plotted for each group. Error bars represent standard error of the mean. *, $P < 0.01$; $n > 100$.

Our study also demonstrates for the first time that phosphorylation of an exocyst component can serve as a mechanism to negatively regulate the exocyst assembly and block exocytosis. How does Cdk1-mediated Exo84 phosphorylation inhibit the assembly of the exocyst complex? Crystallographic studies indicate that most if not all of the exocyst components, including Exo84, have extended rod-like domains composed of α-helical bundles (Dong et al., 2005; Sivaram et al., 2006). It is believed that the "rods" pack adjacent one another to assembly into the holo-exocyst complex (Munson and Novick, 2006). Mass spectrometry analyses showed that Exo84 was phosphorylated by Cdk1 on five residues distributed along the entire Exo84 protein (Ubersax et al., 2003; Loog and Morgan, 2005; Kõivomägi et al., 2011). This is consistent with the observations that Cdks often phosphorylate substrates at multiple positions (Moses et al., 2007a,b; Holt et al., 2009; Enserink and Kolodner, 2010). We speculate that phosphorylation introduces multiple

negative charges along Exo84 that may disturb the otherwise orderly packing of Exo84 with the other exocyst components, thereby disrupting exocyst complex assembly.

In addition to controlling the rate of cell surface expansion, Cdk1 regulates cell morphogenesis, which, in budding yeast, is manifested by bud emergence and polarized daughter cell growth at G1 and S phase. Cdc42 is a master regulator of cell polarity (Park and Bi, 2007). It was shown that Cdc24, the guanine nucleotide exchange factor for Cdc42, is phosphorylated by Cdk1 during G1 phase (McCusker et al., 2007; Wai et al., 2009). In *cdc28* mutant arrested at the G1 phase, the exocyst component Sec3 depolarizes (McCusker et al., 2007). Because the Sec3 is a downstream effector of Cdc42 (Zhang et al., 2001; Zhang et al., 2008), its depolarization is likely mediated through Cdc42 and its associated proteins in the polarity regulation network (Park and Bi, 2007). Consistent with this observation, inhibition of Cdk1 during G1 phase resulted in cell growth defects similar to those caused by actin depolymerization and did not cause a significant accumulation of intracellular vesicles (McCusker et al., 2012). Overall, Cdk1 controls two different aspects of exocytosis (i.e., localization and kinetics) at least at two different stages of the cell cycle (i.e., G1 and M phase).

In summary, our study reveals a molecular mechanism for mitotic arrests during cell growth. As both Cdk1 and the exocyst are evolutionarily conserved, this mechanism is likely to operate in higher eukaryotes. Indeed, the mammalian Exo84 protein contains several putative Cdk1 phosphorylation sites, which suggests that Cdk1-dependent Exo84 regulation is part of a conserved regulatory circuit for growth control. Furthermore, additional proteins in the exocytic pathway may also be affected by CDKs. In the future, it would be interesting to investigate whether Exo84 or other proteins in the secretory pathway are phosphorylated in mammalian cells during mitotic arrest and whether their dephosphorylation contributes to the recovery of membrane expansion, which has been observed at the onset of anaphase (Boucrot and Kirchhausen, 2007). Further investigation of the basic mechanisms of growth control during cell cycle progression is fundamental to advancing our understanding of cell proliferation and cell size homeostasis, both of which are aberrant in a variety of developmental disorders and metabolic diseases.

Materials and methods

Yeast strains, plasmids, and procedures

Standard methods were used for yeast growth and genetic manipulations (Sherman, 2002). All strains used in this project are listed in Table S1. Yeast transformation was performed based on the lithium acetate method (Gietz et al., 1992). 2.5 A_{600} units of early log phase cells were collected in a 1.5-ml centrifuge tube and washed once with 0.5 ml of distilled water. 240 µl PEG 3350 (50% wt/vol), 36 µl 1.0 M LiAc, 5 µl 10 mg/ml sonicated salmon sperm DNA (Agilent Technologies), and 0.1–10 µg DNA were added and the tube was vortexed until the cell pellet had been completely mixed. The cells were then shocked in a water bath at 42°C for 20–25 min. 2–200 µl of the transformation mix was plated onto Petri dish plates containing solid synthetic complete medium. The plates were incubated at 25°C for 2–4 d to recover transformants. Yeast strains containing mutations of the CDK consensus sites were constructed as follows. The balancer plasmid pG279, which contains an Exo84 open reading frame in p416TEF (*URA3, CEN*) plasmid (Mumberg et al., 1995), was transformed into the parental yeast strain, and chromosomal Exo84 was then replaced by KanMX6 according to the procedure described previously (Longtine et al., 1998) and confirmed by sequencing. The *CEN* plasmid contains wild-type *EXO84*, *exo84-A*, or *exo84-E* controlled under the endogenous *EXO84* promoter, and the terminator was transformed into this strain. The transformants were counter-selected for pG279 in medium containing 1 mg/ml 5-fluoroorotic acid. All plasmids used in this study are listed in Table S2. The CDK sites in Exo84 were mutated using a multi-mutagenesis kit (Agilent Technologies).

Whole cell extract preparation

Yeast extracts were prepared using glass beads as described previously (Inagaki et al., 1999). Yeast cells were grown to early log phase and collected by rapid centrifugation. The cell pellet was suspended in ice-cold lysis buffer (50 mM Tris-HCl, pH 7.5, 100 mM NaCl, 1 mM EDTA, 1% Triton X-100, 5 mM NaF, 1 mM sodium pyrophosphate, 1 mM dithiothreitol, and 1× protease inhibitor cocktail; Roche). Glass beads (0.4–0.6 mm in diameter) were added into the resuspended cells. Cells were broken by vigorous vortexing at full speed for 8–10 cycles of 30-s vortexing followed by 30 s in an ice-water bath. The beads and cell debris were removed by centrifugation at 10,000 *g* at 4°C, and the supernatant was further clarified by centrifugation at 100,000 *g* at 4°C. The published Hot-SDS protein extraction protocol was used with slight modifications (Kushnirov, 2000). In brief, 50 A_{600} units of yeast cells were collected by centrifugation, washed once with water, and then suspended in 1 ml of cold distilled water, followed by the addition of 1 ml of 0.2 M NaOH. Samples were mixed and incubated for 5 min at room temperature. Cells were collected by centrifugation, resuspended in 1 ml of SDS sample buffer (0.06 M Tris-HCl, pH 8.6, 5% glycerol, 1% SDS, and 10 mM β-Mercaptoethanol) and boiled for 3–5 min. Samples were centrifuged, and protein concentrations were determined using the DC protein assay kit (Bio-Rad Laboratories).

Secretion assays

Bgl2 secretion assays were performed as previously reported, with modifications (Harsay and Bretscher, 1995). 20 ml of yeast cells were grown to early log phase (OD_{600} is 0.6–1.0) at 25°C. NaN_3 and NaF were added directly to the culture at a final concentration of 10 mM each. 10 OD_{600} units of cells were collected, washed with cell wash buffer (20 mM Tris-HCl, pH 7.5, 10 mM NaN_3, and 10 mM NaF). The cells were resuspended in 300 µl of spheroplast solution buffer (50 mM Tris-HCl, pH 7.5, 1.4 M sorbitol, 10 mM NaN_3, 10 mM NaF, 30 mM 2-Mercaptoethanol, and 0.2 mg/ml Zymolyase) and incubated at 37°C in a water bath for 30 min. The spheroplasts were pelleted gently by centrifuge at 2,000 rpm for 5 min at 4°C. 100 µl of supernatant was carefully transferred to a new tube and mixed with 20 µl of 6× SDS loading buffer (300 mM Tris-HCl, pH 6.8, 600 mM dithiothreitol, 12% SDS, 0.6% bromophenol blue, and 60% glycerol). This is the external pool. The remaining supernatant was removed and the pellet (spheroplasts) was washed once with 1 ml of spheroplast wash buffer (50 mM Tris-HCl, pH 7.5, 1.4 M sorbitol, 10 mM NaN_3, and 10 mM NaF) to remove residue external pool. The spheroplasts were dissolve in 300 µl of lysate buffer (20 mM Tris-HCl, pH 7.5, 100 mM NaCl, 2 mM $MgCl_2$, 0.5% Triton X-100, and 1× protease inhibitor cocktail; Roche) by leaving on ice for 10 min. The cell debris was removed after the sample was centrifuged at 13,000 rpm for 5 min at 4°C. 100 µl of supernatant (lysates) was transferred to a new tube and mixed with 20 µl of 6× SDS loading buffer. This is the internal pool. The internal pool and external pool samples were boiled at 95°C for 5 min, loaded into 12% SDS-PAGE gel. Bgl2 was detected by Western blotting with an anti-Bgl2 rabbit polyclonal antibody (1:2,000). For temperature-sensitive mutants, the cells were grown at 25°C or shifted to 37°C for 90 min before being processed for the Bgl2 assay. For cells arrested at metaphase by nocodazole, the cells were treated with DMSO or 15 µg/ml nocodazole for 3 h before being processed for secretion assays.

Invertase secretion was examined as described previously (Novick et al., 1980). 20 ml of yeast cells were grown to early log phase (OD_{600} is 0.6–1.0) at 25°C. 1 OD cells were transferred to a new tube and washed with 1 ml of ice cold 1 mM NaN_3. The cells were then resuspended in 1 ml YP plus glucose medium (1% Bacto-yeast, 2% Bactopeptone, and 0.1% glucose) and incubated at 25°C for 1 h to induce invertase expression. After 1 h of incubation, the cells were collected and washed once with 1 ml 10 mM NaN_3. The cells were resuspended in 1 ml 10mM NaN_3 and kept on ice. The external invertase was measured directly on the whole intact cells, whereas the internal invertase was measured after preparation of lysates. 0.5 ml of cells were removed and mixed with 0.5 ml of 2× spheroplast cocktail mix (2.8 M sorbitol, 0.1 M Tris-HCl pH 7.5, 10 mM NaN3, 0.4% 2-Mercaptoethanol, and 10 µg/ml Zymolyase-100T). The cells were incubated in water bath at 37°C for

45 min. The spheroplasts were collected and the supernatant was removed carefully without disturbing the pellet. The spheroplasts were dissolved at 4°C in 0.5 ml 0.5% Triton X-100. The invertase assay was performed in 13 × 100 mm tubes. 20 µl of sample was placed in the tube and 80 µl of 50 mM NaAc, pH 5.1, was added. Then 25 µl of 0.5 M sucrose was added and the tube was incubated at 37°C for 30 min. 150 µl of 0.2 M K_2HPO_4 was added and the tube was placed on ice to stop the reaction. The sample was boiled for 3 min and put on ice. 1 ml of assay mix was added (0.1 M KPi buffer, pH 7.0, 10 U/ml glucose oxidase, 2.5 µg/ml peroxidase, 150 µg/ml *O*-dianisidine, and 20 µM *N*-Ethylmaleimide) and the sample was incubated at 37°C for 30 min. 1 ml of 6 N HCl was added into the tube and the value of A540 was measured by the Spectrophotometer (SmartSpec 3000; Bio-Rad Laboratories). For temperature-sensitive mutants, the cells were grown at 25°C or shifted to 37°C for 90 min and then were grown in low-glucose medium (0.1% glucose) at the same temperature for 1 h.

Glycoprotein secretion assays were performed as described previously (Zhang et al., 2005). For temperature-sensitive mutants, the cells were grown to early log phase. The cultures were then collected, washed, and resuspended in the fresh medium and grown at 25°C or shifted to 37°C for 60 min. The supernatant was mixed with 2% (wt/vol) sodium deoxycholate and incubated for 30 min on ice. Samples were precipitated with 100% (wt/vol) trichloroacetic acid, followed by a 1-h incubation on ice. The trichloroacetic acid–precipitated proteins were then washed twice with acetone, air-dried, and dissolved into the loading buffer (125 mM Tris-HCl, pH 6.8, 4% SDS, 20% [vol/vol] glycerol, and 5% 2-Mercaptoethanol) for SDS-PAGE. The Schiff's reagent (Sigma-Aldrich) staining for SDS-PAGE gel was performed as described previously (Zhang et al., 2005). The gel was fixed in a solution containing 10% acetic acid and 40% ethanol for at least 30 min and up to overnight, and then incubated in 7.5% acetic acid for 10 min and 1% periodic acid (wt/vol) for 15 min after washing with distilled water six times for 5 min each. The gel was incubated in Schiff reagent for 15 min and washed with water briefly. After that, the stained gel was washed with freshly prepared 0.5% sodium metabisulfite three times for 10 min each. Finally, the gel was washed with distilled water at least six times until excess stain was removed. For the glycoprotein secretion assay during the cell cycle after α-factor release, cells were arrested at G1 phase by 1 µg/ml α-factor for 3.5 h and then released into fresh medium. At time points 30 min and 90 min, 50 ml of the culture was collected, washed, and resuspended in the fresh medium. After incubation for 10 min, the glycoproteins were then processed for SDS-PAGE and Schiff's reagent staining.

Immunoprecipitation and detection of Exo84 phosphorylation

For immunoprecipitation of myc-tagged Exo84, total proteins were extracted by using the glass beads method (Inagaki et al., 1999). A mouse anti-myc antibody (9E10) or rabbit anti-Exo84 antibody was used for immunoprecipitation. Typically, 50 A_{600} units of a mid-log phase yeast culture were harvested and total protein was extracted using Hot-SDS protein extraction method (Kushnirov, 2000). Cell lysates were used for immunoprecipitation using protein G beads and anti-myc antibody (9E10) in immunoprecipitation buffer (50 mM Tris-HCl, pH 7.5, 150 mM NaCl, 1 mM EDTA, 1 mM EGTA, 10% glycerol, and 1× protease inhibitor; Roche) and 1× phosphatase inhibitor I (Roche) at 4°C for 4 h with rotation. Beads were washed with washing buffer (50 mM Tris-HCl, pH 7.5, 150 mM NaCl, 1 mM EDTA, 1 mM EGTA, and 10% glycerol) three times. The beads were mixed with 30 µl of 1× SDS loading buffer and incubated at 95°C for 5 min. Protein samples were then cooled on ice for several minutes and separated on 10% SDS-PAGE gel. Western blotting was performed using the phospho–CDK substrate antibody (Molecular Probes) and anti-Exo84 antibody. Phos-tag PAGE gel was used to detect the phosphorylation of Exo84 during the cell cycle. The final concentration of phos-tag (Wako Pure Chemical Industries, Ltd.) is 5 µM and the Western blot was performed as described previously (Kinoshita et al., 2009). The Images were further processed using ImageJ software (National Institutes of Health).

λ-Phosphatase treatment

Where designated, immunoprecipitated protein complexes were treated with λ protein phosphatase as described by the supplier (P0753S; New England Biolabs, Inc.).

In vitro Cdk1 kinase assays

Cln2–Cdk1, Clb5–Cdk1, and Clb2–Cdk1 kinase complexes were purified as described previously (Loog and Morgan, 2005; McCusker et al., 2007). 50-µl reactions were prepared in kinase assay buffer (50 mM Hepes, pH 7.5, 2 mM $MgCl_2$, 0.05% Tween-20, 2.5% glycerol, 1 mM DTT, and 1 mM ATP) containing 7 nM of Cln2–Cdk1, Clb5–Cdk1, or Clb2–Cdk1 and 1 µg GST or 2 µg GST-Exo84 fusion protein, 10 µCi γ-[^{32}P]ATP. Reactions were incubated at room temperature for 60 min and terminated by the addition of 10 µl of 6× sample buffer. Samples were resolved on 10% SDS–PAGE gel. The ^{32}P radioactive signal was analyzed by autoradiography.

Microscopy

Fluorescence microscopy was conducted with a fluorescence microscope (CTR6000; Leica) equipped with a Plan-Apochromat 100×, 1.40 NA oil immersion objective lens. Images were taken using LAS AF 1.5.1 acquisition software (Leica). Determination of the cell cycle stages was performed by surveying nuclear position and morphology using a MARS-tagged nuclear envelope protein (Nup57-MARS) as described previously (Khmelinskii et al., 2010). The yeast strains harboring both Sec5-3×GFP and Nup57-MARS on the chromosome were grown to early log phase in synthetic complete (SC) medium overnight at 25°C. Samples were collected by centrifugation and resuspended in fresh SC medium. Slides containing agar pads were prepared with 2% agar dissolved in SC medium containing the appropriate amino acids. 2 µl of the suspension was dropped onto the agar pad, and a coverslip was placed on top of the pad. Images were captured with a digital camera (DFC350FX; Leica) at room temperature every 2 min with 0.25 s of exposure time. For each time point, the background intensity was subtracted and the images from different channels were merged using ImageJ software.

For EM, cells were collected by vacuum filtration using a 0.45 µm nitrocellulose membrane and were fixed for 1 h at room temperature in 0.1 M cacodylate, pH 7.4, 3% formaldehyde, 1 mM $MgCl_2$, and 1 mM $CaCl_2$. The cells were spheroplasted and fixed with 1% glutaraldehyde (in PBS, pH 7.4) at 4°C overnight. The spheroplasts were washed in 0.1 M cacodylate buffer and were postfixed twice with ice-cold 0.5% OsO_4 and 0.8% potassium for 10 min each. After dehydration and embedding in Spurr's epoxy resin (Polysciences, Inc.), thin sections were cut and transferred onto 600 mesh uncoated copper grids (Ernest Fullam, Inc.) and were poststained with uranyl acetate and lead citrate. Cells were observed on a transmission electron microscope (Model 1010; JEOL) at 100,000× magnification. Electronic microscopy with permanganate fixation was performed according to the procedure described previously (Perkins and McCaffery, 2007). Yeast strains were grown in YPD (1% Bacto-yeast, 2% Bacto-peptone, and 2% glucose) overnight to early log phase. Cells were collected and resuspended in 100 mM sodium cacodylate, pH 7.4, containing 3% glutaraldehyde, 5 mM $CaCl_2$, and 5 mM $MgCl_2$, for 1 h. The samples were washed with 100 mM sodium cacodylate, pH 7.4, embedded in ultra-low-temperature gelling agarose, and cut into small pieces. These blocks were postfixed in 4% $KMNO_4$ for 1 h and then washed thoroughly in double-distilled water. The samples were treated with 0.5% sodium meta-periodate for 15 min and washed with double-distilled water. After that, the samples were treated with 2% uranyl acetate overnight, dehydrated through a graded series of ethanol (50–100%, ice cold), and followed by two washes with propylene oxide. The samples were resuspended in the mixture of propylene oxide and Spurr resin (1:1) and rotated overnight, transferred to 100% Spurr resin, and left in a vacuum for 24 h. The next day, the resin was changed three times and the samples were then rotated overnight. Subsequently, the samples were put in BEEM capsules containing fresh Spurr resin and put in the oven at 65°C for 48 h. Sections were cut, placed onto 400-mesh nickel grids, and poststained with lead citrate for 2 min

In vitro transcription/translation

DNA templates for in vitro transcription/translation were generated by PCR and subcloned into mammalian expression vectors containing a cytomegalovirus (CMV) promoter. [^{35}S]cysteine/methionine-labeled proteins were generated with an in vitro transcription/translation kit according to the manufacturer's instructions (Promega). For binding experiments, the proteins to be tested for binding were cotranscribed/translated in vitro. After the reaction, 3 µl of the reaction mixture were diluted 100-fold into the binding buffer for in vitro binding assays.

Online supplemental materials

Fig. S1 shows that secretion of Bgl2 was blocked in metaphase-arrested *cdc23-1* mutant cells and that invertase secretion was not changed in *cdc* mutants. Fig. S2 shows measurement of exocytosis in cells arrested at metaphase by nocodazole treatment. Fig. S3 shows that Cdk1 activity is required for Exo84 phosphorylation, exocyst assembly, and block of Bgl2 secretion at metaphase. Fig. S4 shows the time-lapse fluorescence microscopy of Exo84 wild-type and phosphorylation mutant cells during mitosis.

Tables S1 and S2 show yeast strains and plasmids used in this study, respectively. Online supplemental material is available at http://www.jcb.org/cgi/content/full/jcb.201211093/DC1.

We thank Drs. Jorrit Enserink, Alexi Goranov, Angelika Amon, Derek McCusker, Douglas Kellogg, and Erfei Bi for reagents and helpful discussions.

This work is supported by a grant from the National Institute of General Medical Sciences (GM085146) to W. Guo.

Submitted: 16 November 2012
Accepted: 4 June 2013

References

Adamo, J.E., J.J. Moskow, A.S. Gladfelter, D. Viterbo, D.J. Lew, and P.J. Brennwald. 2001. Yeast Cdc42 functions at a late step in exocytosis, specifically during polarized growth of the emerging bud. *J. Cell Biol.* 155:581–592. http://dx.doi.org/10.1083/jcb.200106065

Albuquerque, C.P., M.B. Smolka, S.H. Payne, V. Bafna, J. Eng, and H. Zhou. 2008. A multidimensional chromatography technology for in-depth phosphoproteome analysis. *Mol. Cell. Proteomics*. 7:1389–1396. http://dx.doi.org/10.1074/mcp.M700468-MCP200

Bishop, A.C., J.A. Ubersax, D.T. Petsch, D.P. Matheos, N.S. Gray, J. Blethrow, E. Shimizu, J.Z. Tsien, P.G. Schultz, M.D. Rose, et al. 2000. A chemical switch for inhibitor-sensitive alleles of any protein kinase. *Nature*. 407:395–401. http://dx.doi.org/10.1038/35030148

Boucrot, E., and T. Kirchhausen. 2007. Endosomal recycling controls plasma membrane area during mitosis. *Proc. Natl. Acad. Sci. USA*. 104:7939–7944. http://dx.doi.org/10.1073/pnas.0702511104

Boucrot, E., and T. Kirchhausen. 2008. Mammalian cells change volume during mitosis. *PLoS ONE*. 3:e1477. http://dx.doi.org/10.1371/journal.pone.0001477

Bryant, D.M., and K.E. Mostov. 2008. From cells to organs: building polarized tissue. *Nat. Rev. Mol. Cell Biol.* 9:887–901. http://dx.doi.org/10.1038/nrm2523

Dong, G., A.H. Hutagalung, C. Fu, P. Novick, and K.M. Reinisch. 2005. The structures of exocyst subunit Exo70p and the Exo84p C-terminal domains reveal a common motif. *Nat. Struct. Mol. Biol.* 12:1094–1100. http://dx.doi.org/10.1038/nsmb1017

Enserink, J.M., and R.D. Kolodner. 2010. An overview of Cdk1-controlled targets and processes. *Cell Div.* 5:11. http://dx.doi.org/10.1186/1747-1028-5-11

Erickson, C.A., and J.P. Trinkaus. 1976. Microvilli and blebs as sources of reserve surface membrane during cell spreading. *Exp. Cell Res.* 99:375–384. http://dx.doi.org/10.1016/0014-4827(76)90595-4

Gietz, D., A. St Jean, R.A. Woods, and R.H. Schiestl. 1992. Improved method for high efficiency transformation of intact yeast cells. *Nucleic Acids Res.* 20:1425. http://dx.doi.org/10.1093/nar/20.6.1425

Goranov, A.I., and A. Amon. 2010. Growth and division—not a one-way road. *Curr. Opin. Cell Biol.* 22:795–800. http://dx.doi.org/10.1016/j.ceb.2010.06.004

Goranov, A.I., M. Cook, M. Ricicova, G. Ben-Ari, C. Gonzalez, C. Hansen, M. Tyers, and A. Amon. 2009. The rate of cell growth is governed by cell cycle stage. *Genes Dev.* 23:1408–1422. http://dx.doi.org/10.1101/gad.1777309

Guo, W., A. Grant, and P. Novick. 1999. Exo84p is an exocyst protein essential for secretion. *J. Biol. Chem.* 274:23558–23564. http://dx.doi.org/10.1074/jbc.274.33.23558

Guo, W., M. Sacher, J. Barrowman, S. Ferro-Novick, and P. Novick. 2000. Protein complexes in transport vesicle targeting. *Trends Cell Biol.* 10:251–255. http://dx.doi.org/10.1016/S0962-8924(00)01754-2

Hall, A., and G. Lalli. 2010. Rho and Ras GTPases in axon growth, guidance, and branching. *Cold Spring Harb. Perspect. Biol.* 2:a001818. http://dx.doi.org/10.1101/cshperspect.a001818

Harsay, E., and A. Bretscher. 1995. Parallel secretory pathways to the cell surface in yeast. *J. Cell Biol.* 131:297–310. http://dx.doi.org/10.1083/jcb.131.2.297

Harsay, E., and R. Schekman. 2002. A subset of yeast vacuolar protein sorting mutants is blocked in one branch of the exocytic pathway. *J. Cell Biol.* 156:271–285. http://dx.doi.org/10.1083/jcb.200109077

He, B., and W. Guo. 2009. The exocyst complex in polarized exocytosis. *Curr. Opin. Cell Biol.* 21:537–542. http://dx.doi.org/10.1016/j.ceb.2009.04.007

He, B., F. Xi, J. Zhang, D. TerBush, X. Zhang, and W. Guo. 2007. Exo70p mediates the secretion of specific exocytic vesicles at early stages of the cell cycle for polarized cell growth. *J. Cell Biol.* 176:771–777. http://dx.doi.org/10.1083/jcb.200606134

Holm, C., T. Goto, J.C. Wang, and D. Botstein. 1985. DNA topoisomerase II is required at the time of mitosis in yeast. *Cell*. 41:553–563. http://dx.doi.org/10.1016/S0092-8674(85)80028-3

Holt, L.J., B.B. Tuch, J. Villén, A.D. Johnson, S.P. Gygi, and D.O. Morgan. 2009. Global analysis of Cdk1 substrate phosphorylation sites provides insights into evolution. *Science*. 325:1682–1686. http://dx.doi.org/10.1126/science.1172867

Hsu, S.C., D. TerBush, M. Abraham, and W. Guo. 2004. The exocyst complex in polarized exocytosis. *Int. Rev. Cytol.* 233:243–265. http://dx.doi.org/10.1016/S0074-7696(04)33006-8

Inagaki, M., T. Schmelzle, K. Yamaguchi, K. Irie, M.N. Hall, and K. Matsumoto. 1999. PDK1 homologs activate the Pkc1-mitogen-activated protein kinase pathway in yeast. *Mol. Cell. Biol.* 19:8344–8352.

Jorgensen, P., and M. Tyers. 2004. How cells coordinate growth and division. *Curr. Biol.* 14:R1014–R1027. http://dx.doi.org/10.1016/j.cub.2004.11.027

Khmelinskii, A., P.J. Keller, H. Lorenz, E. Schiebel, and M. Knop. 2010. Segregation of yeast nuclear pores. *Nature*. 466:E1. http://dx.doi.org/10.1038/nature09255

Kinoshita, E., E. Kinoshita-Kikuta, and T. Koike. 2009. Separation and detection of large phosphoproteins using Phos-tag SDS-PAGE. *Nat. Protoc.* 4:1513–1521. http://dx.doi.org/10.1038/nprot.2009.154

Kõivomägi, M., E. Valk, R. Venta, A. Iofik, M. Lepiku, D.O. Morgan, and M. Loog. 2011. Dynamics of Cdk1 substrate specificity during the cell cycle. *Mol. Cell*. 42:610–623. http://dx.doi.org/10.1016/j.molcel.2011.05.016

Kreiner, T., and H.P. Moore. 1990. Membrane traffic between secretory compartments is differentially affected during mitosis. *Cell Regul.* 1:415–424.

Kushnirov, V.V. 2000. Rapid and reliable protein extraction from yeast. *Yeast*. 16:857–860. http://dx.doi.org/10.1002/1097-0061(20000630)16:9<857::AID-YEA561>3.0.CO;2-B

Leaf, D.S., S.J. Roberts, J.C. Gerhart, and H.P. Moore. 1990. The secretory pathway is blocked between the trans-Golgi and the plasma membrane during meiotic maturation in *Xenopus oocytes*. *Dev. Biol.* 141:1–12. http://dx.doi.org/10.1016/0012-1606(90)90097-3

Lim, H.H., P.Y. Goh, and U. Surana. 1998. Cdc20 is essential for the cyclosome-mediated proteolysis of both Pds1 and Clb2 during M phase in budding yeast. *Curr. Biol.* 8:231–234. http://dx.doi.org/10.1016/S0960-9822(98)70088-0

Liu, J., and W. Guo. 2012. The exocyst complex in exocytosis and cell migration. *Protoplasma*. 249:587–597. http://dx.doi.org/10.1007/s00709-011-0330-1

Longtine, M.S., A. McKenzie III, D.J. Demarini, N.G. Shah, A. Wach, A. Brachat, P. Philippsen, and J.R. Pringle. 1998. Additional modules for versatile and economical PCR-based gene deletion and modification in *Saccharomyces cerevisiae*. *Yeast*. 14:953–961. http://dx.doi.org/10.1002/(SICI)1097-0061(199807)14:10<953::AID-YEA293>3.0.CO;2-U

Loog, M., and D.O. Morgan. 2005. Cyclin specificity in the phosphorylation of cyclin-dependent kinase substrates. *Nature*. 434:104–108. http://dx.doi.org/10.1038/nature03329

Lowe, M., N. Nakamura, and G. Warren. 1998. Golgi division and membrane traffic. *Trends Cell Biol.* 8:40–44. http://dx.doi.org/10.1016/S0962-8924(97)01189-6

Lucocq, J.M., and G. Warren. 1987. Fragmentation and partitioning of the Golgi apparatus during mitosis in HeLa cells. *EMBO J.* 6:3239–3246.

Makarow, M. 1988. Secretion of invertase in mitotic yeast cells. *EMBO J.* 7:1475–1482.

McCusker, D., and D.R. Kellogg. 2012. Plasma membrane growth during the cell cycle: unsolved mysteries and recent progress. *Curr. Opin. Cell Biol.* 24:845–851. http://dx.doi.org/10.1016/j.ceb.2012.10.008

McCusker, D., C. Denison, S. Anderson, T.A. Egelhofer, J.R. Yates III, S.P. Gygi, and D.R. Kellogg. 2007. Cdk1 coordinates cell-surface growth with the cell cycle. *Nat. Cell Biol.* 9:506–515. http://dx.doi.org/10.1038/ncb1568

McCusker, D., A. Royou, C. Velours, and D.R. Kellogg. 2012. Cdk1-dependent control of membrane-trafficking dynamics. *Mol. Biol. Cell*. 23:3336–3347. http://dx.doi.org/10.1091/mbc.E11-10-0834

Mendenhall, M.D., and A.E. Hodge. 1998. Regulation of Cdc28 cyclin-dependent protein kinase activity during the cell cycle of the yeast *Saccharomyces cerevisiae*. *Microbiol. Mol. Biol. Rev.* 62:1191–1243.

Mitchison, J.M., and P. Nurse. 1985. Growth in cell length in the fission yeast *Schizosaccharomyces pombe*. *J. Cell Sci.* 75:357–376.

Moses, A.M., J.K. Hériché, and R. Durbin. 2007a. Clustering of phosphorylation site recognition motifs can be exploited to predict the targets of cyclin-dependent kinase. *Genome Biol.* 8:R23. http://dx.doi.org/10.1186/gb-2007-8-2-r23

Moses, A.M., M.E. Liku, J.J. Li, and R. Durbin. 2007b. Regulatory evolution in proteins by turnover and lineage-specific changes of cyclin-dependent

kinase consensus sites. *Proc. Natl. Acad. Sci. USA*. 104:17713–17718. http://dx.doi.org/10.1073/pnas.0700997104

Mumberg, D., R. Müller, and M. Funk. 1995. Yeast vectors for the controlled expression of heterologous proteins in different genetic backgrounds. *Gene*. 156:119–122. http://dx.doi.org/10.1016/0378-1119(95)00037-7

Munson, M., and P. Novick. 2006. The exocyst defrocked, a framework of rods revealed. *Nat. Struct. Mol. Biol.* 13:577–581. http://dx.doi.org/10.1038/nsmb1097

Nelson, W.J., and C. Yeaman. 2001. Protein trafficking in the exocytic pathway of polarized epithelial cells. *Trends Cell Biol.* 11:483–486. http://dx.doi.org/10.1016/S0962-8924(01)02145-6

Novick, P., C. Field, and R. Schekman. 1980. Identification of 23 complementation groups required for post-translational events in the yeast secretory pathway. *Cell*. 21:205–215. http://dx.doi.org/10.1016/0092-8674(80)90128-2

Park, H.O., and E. Bi. 2007. Central roles of small GTPases in the development of cell polarity in yeast and beyond. *Microbiol. Mol. Biol. Rev.* 71:48–96. http://dx.doi.org/10.1128/MMBR.00028-06

Peng, Y., and L.S. Weisman. 2008. The cyclin-dependent kinase Cdk1 directly regulates vacuole inheritance. *Dev. Cell*. 15:478–485. http://dx.doi.org/10.1016/j.devcel.2008.07.007

Perkins, E.M., and J.M. McCaffery. 2007. Conventional and immunoelectron microscopy of mitochondria. *Methods Mol. Biol.* 372:467–483. http://dx.doi.org/10.1007/978-1-59745-365-3_33

Prescott, D.M., and M.A. Bender. 1962. Synthesis of RNA and protein during mitosis in mammalian tissue culture cells. *Exp. Cell Res.* 26:260–268. http://dx.doi.org/10.1016/0014-4827(62)90176-3

Quinlan, R.A., C.I. Pogson, and K. Gull. 1980. The influence of the microtubule inhibitor, methyl benzimidazol-2-yl-carbamate (MBC) on nuclear division and the cell cycle in *Saccharomyces cerevisiae*. *J. Cell Sci.* 46:341–352.

Seemann, J., M. Pypaert, T. Taguchi, J. Malsam, and G. Warren. 2002. Partitioning of the matrix fraction of the Golgi apparatus during mitosis in animal cells. *Science*. 295:848–851. http://dx.doi.org/10.1126/science.1068064

Shaw, S.L., P. Maddox, R.V. Skibbens, E. Yeh, E.D. Salmon, and K. Bloom. 1998. Nuclear and spindle dynamics in budding yeast. *Mol. Biol. Cell*. 9:1627–1631.

Sherman, F. 2002. Getting started with yeast. *Methods Enzymol.* 350:3–41. http://dx.doi.org/10.1016/S0076-6879(02)50954-X

Sivaram, M.V.S., M.L.M. Furgason, D.N. Brewer, and M. Munson. 2006. The structure of the exocyst subunit Sec6p defines a conserved architecture with diverse roles. *Nat. Struct. Mol. Biol.* 13:555–556. http://dx.doi.org/10.1038/nsmb1096

Smolka, M.B., C.P. Albuquerque, S.H. Chen, and H. Zhou. 2007. Proteome-wide identification of in vivo targets of DNA damage checkpoint kinases. *Proc. Natl. Acad. Sci. USA*. 104:10364–10369. http://dx.doi.org/10.1073/pnas.0701622104

Tzur, A., R. Kafri, V.S. LeBleu, G. Lahav, and M.W. Kirschner. 2009. Cell growth and size homeostasis in proliferating animal cells. *Science*. 325:167–171. http://dx.doi.org/10.1126/science.1174294

Ubersax, J.A., E.L. Woodbury, P.N. Quang, M. Paraz, J.D. Blethrow, K. Shah, K.M. Shokat, and D.O. Morgan. 2003. Targets of the cyclin-dependent kinase Cdk1. *Nature*. 425:859–864. http://dx.doi.org/10.1038/nature02062

Wai, S.C., S.A. Gerber, and R. Li. 2009. Multisite phosphorylation of the guanine nucleotide exchange factor Cdc24 during yeast cell polarization. *PLoS ONE*. 4:e6563. http://dx.doi.org/10.1371/journal.pone.0006563

Whyte, J.R.C., and S. Munro. 2002. Vesicle tethering complexes in membrane traffic. *J. Cell Sci.* 115:2627–2637.

Zachariae, W., and K. Nasmyth. 1999. Whose end is destruction: cell division and the anaphase-promoting complex. *Genes Dev.* 13:2039–2058. http://dx.doi.org/10.1101/gad.13.16.2039

Zhang, X., E. Bi, P. Novick, L. Du, K.G. Kozminski, J.H. Lipschutz, and W. Guo. 2001. Cdc42 interacts with the exocyst and regulates polarized secretion. *J. Biol. Chem.* 276:46745–46750. http://dx.doi.org/10.1074/jbc.M107464200

Zhang, X., A. Zajac, J. Zhang, P. Wang, M. Li, J. Murray, D. TerBush, and W. Guo. 2005. The critical role of Exo84p in the organization and polarized localization of the exocyst complex. *J. Biol. Chem.* 280:20356–20364. http://dx.doi.org/10.1074/jbc.M500511200

Zhang, X., K. Orlando, B. He, F. Xi, J. Zhang, A. Zajac, and W. Guo. 2008. Membrane association and functional regulation of Sec3 by phospholipids and Cdc42. *J. Cell Biol.* 180:145–158. http://dx.doi.org/10.1083/jcb.200704128